CHALMERS
UNIVERSITY OF TECHNOLOGY

Experimental study on charging materials interfaces inside HVAC cable termination

Master's thesis in Electric Power Engineering

PHILIP HOANG

Department of Electrical Engineering
CHALMERS UNIVERSITY OF TECHNOLOGY
Gothenburg, Sweden 2020

Master's thesis

Experimental study on charging materials interfaces inside HVAC cable termination

Philip Hoang

CHALMERS
UNIVERSITY OF TECHNOLOGY

Department of Electrical Engineering
Division of Electric Power Engineering
Chalmers University of Technology
Gothenburg, Sweden 2020

Experimental study on charging materials interfaces inside HVAC cable termination
PHILIP HOANG

Supervisor: Sarath Kumara, Department of Electrical Engineering
Examiner: Yuriy Serdyuk, Department Electrical Engineering

Master's Thesis
Department of Electrical Engineering
Division of Electric Power Engineering
Chalmers University of Technology
SE-412 96 Gothenburg
Telephone +46 31 772 1000

Typeset in LaTeX
Gothenburg, Sweden 2020

Experimental study on charging materials interfaces inside HVAC cable termination
Philip Hoang
Department of Electrical Engineering
Chalmers University of Technology

Abstract

The high voltage alternative current (HVAC) cable termination business is under a transition from liquid filled applications to dry applications using a gelatinous insulation polymer (silicone gel). Currently, cable terminations for voltages up to 145 kV are available on the market. For higher voltage levels, the technology is under development. Thus it has been found during large scale impulse testing that using conventional design principles for devices intendent to operate at high voltages led to unacceptable rate of failure. To understand the failure mechanism and to suggest solutions for improving the existing design, experimental investigations were conducted focusing on charging of internal interfaces in the insulation. The experimental set-up has been developed and built including test cells, a measuring system consisting of an electrostatic voltmeter equipped with a surface potential probe, positioning system for surface scanning and data acquisition system. To convert measured surface potential data to respective surface charge densities, computer simulations based Comsol Multiphysics software have been implemented. In the experiments, different methodologies were used to localize the surface charge inside the HVAC cable termination and for electrical characterization of the insulating gel. Thus, insulation surface charging from external corona discharge and by pre-stressing with a test voltage were implemented. The obtained results indicated weak dependence of the electric conductivity of the gel and its stability in time that make surface charge accumulation been essential. The surface potential/charge decay characteristics obtained in the test cell, which mimics the actual HVAC cable termination, confirmed this finding and thus indicated that surface charging of internal interfaces in the dry termination may be responsible for the failures observed during impulse testing. From the design perspective, this study emphasizes the importance of the charging behavior of the dry cable terminations, which should be taken into consideration for further development of the technology.

Keywords: Corona Charging, Charge Decay, POWERSIL, Surface Charge, HVAC Cable Termination, Charging behaviour, Charge Dynamics.

Preface and Acknowledgements

This thesis report is the concluding piece of the Master's programme Electrical Power Engineering at Chalmers University of Technology. It was carried out in the middle of the COVID-19 pandemic from the beginning of January 2020 to early autumn 2020 in a close collaboration with cable manufacturing company NKT.

First and foremost I would like to express my sincere appreciation and gratitude towards my examiner Prof.Yuriy Serdyuk and supervisor PhD. Sarath Kumara for their guidance and expertise in this field. Many thanks to PhD. Lei Chen and PhD. David Kiefer at NKT for their support and engagement in this project. I would also like to pay a mentioning to Adj.Prof. Olof Hjortstam for his valuable inputs into this project, Sun Chenxuan for his helping of building the laboratory setup and good discussion in parallel with his work. Thanks once again for the opportunity to have an insight of the work of a researcher

Last but not least I would like to thank my family for all the moral support, always believing and encouraging me since I was a little kid.

Philip Hoang, Gothenburg, September 2020

Contents

List of Figures

List of Tables

1
Introduction

The high voltage alternative current (HVAC) cable termination business is under a transition from liquid filled applications to dry applications. The existing dry cable termination technology developed by NKT, using a stress cone and a silicone compound as known as POWERSIL gel between the stress cone and the outer insulator, has been commercialized up to 145 kV. During NKT's development project, a static electric field calculation was made along the polymeric surfaces inside the termination. In order to develop the dry termination for higher voltage levels where the requirement on electric strength is much higher, a better understanding of charging behavior along the surfaces of silicone compounds is needed, so that the electric field distribution can be better controlled to avoid breakdown triggered by lightning impulse. In addition to advanced E-field calculation, it will be necessary to build up small scale test facility to prove the concept via down scaled testing. The objective of this master thesis work is to build up lab scale test facility and execute measurement on simplified and down scaled termination configuration to verify the E-field distribution from the calculation and optimize the termination design for higher voltage level.

1.1 Background

The market success of NKT's first dry cable termination resulted in an aim for even higher voltage classes. However, for higher voltages some electric breakdown appears due to surface charges between the polymeric insulation material and the air boundary. In ideal cases the surface of the gel is totally flat against the air, but due to thermal shifting and pressure fluctuation, the insulation material may be compressed and thus forms a curved surface. This surface geometry contributes to some sharp geometries around the edges of the polymeric material, air and the termination casing. NKT has done static calculation on electric field strength along polymeric surfaces inside the cable termination. The calculation results indicated an uneven E-field strength distribution along various zones, where the most critical areas with much concentrated field strength can be found. The most critical area with highly concentrated field strength was then concluded to be the location where electric breakdown happened, which led to the failure of whole termination during a standardised lightning impulse test according to specific IEC standard. Following Figure 1.1 illustrates the structure of the cable termination that is in the projects interest.

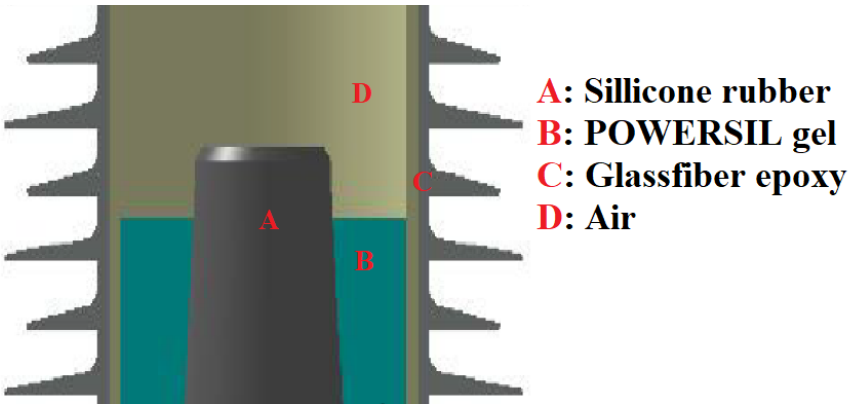

Figure 1.1: Detailed illustration inside a gel-filled cable termination [1]

1.2 Aim

The aim of the work is to understand the charge dynamics on the polymeric insulation gel inside a cable termination.

1.3 Objectives

The following objectives of this project can be concluded to these following bulletin points;

- Build up lab scale test setup including power source, test cell, measurement instrument.
- Conduct experiments on grounded flat gel sample
- Execute experiment with test cell using
  - Corona charging through needle
  - Energized electrode behind SiR plate
- Collect empirical data from measurements
- Simulate response function of probe and construct test cell in COMSOL for calculation
- Convert and calculate the surface charge density
- Perform field calculations based on the results
- Compare and evaluate the results

1.4 Limitations

These following limitations will not be touched upon this report,

- Temperature shift, since the pressure is mainly affected by thermal expansion of the surrounding material. Therefore pressure will be applied by external force instead.
- Moisture & humidity condition, since the application of the material is enclosed in cable termination, therefore only dry condition will be dealt with in this project.

- Control of ions in the air will not be taken into consideration, which means the density of ions will be randomized each day.

2
Theory

For this project, knowledge about charge decay mechanism, estimation charge density and charge injection are needed. This chapter will cover all these fundamental physics and knowledge related to the experiments.

2.1 Charging of polymeric surfaces

In order to test out the electrical stresses that occur on the polymeric material, an appliance of charges has to be made. This section describe different methods of obtaining surface charge on the material in relevance to this project.

2.1.1 Corona charging in gaseous dielectric

Corona charging is a self sustainable and non disruptive electric discharge that allows charging between asymmetrical surfaces such as needle-plane, rod-plane or needle-rod if sufficient potential difference is acquired [3]. The cause of corona discharges is due to its strong inhomogeneous electric field distribution from the sharp edge of electrode. the discharge is located at the very sharpest surface of the electrode under such field condition, so called ionizing region. The ionizing region is where the highest concentration of E-field is, making ionization of gas easily creating positive charged ions propagating towards the grounded element. This method allows injection of charges when placing a material between electrode and grounded element.

2.1.2 Pre-stressing

Pre-stressing of an insulating material is when AC or DC-voltage is applied below the breakdown voltage level. The charging of the material could be from charge injection, internal discharges, polarisation of materials. For DC stressing, the voltage is slowly raised up to wanted voltage level before setting at steady state. The field between the insulator and electrode is varying during the charging stage i.e. During the raising of the voltage, the field is of capacitive characteristic due to the change of voltage over time. After a while into steady state, the E-field becomes more resistive type [4]. In some cases the pre-stressing could initiate corona discharges if the voltage level is sufficient. the discharges could be located at either existing triple junction or near the electrode if sharp edges are exposed. On the latter statement, charge injection could occur if the electrode edge is angled towards the insulator.

This can be mitigated by constructing a more suitable electrode for the application or compensate for the strong field around that area.

2.2 Charge decay mechanism

This section will present the different charge decay mechanisms, such as bulk decay, surface decay and gaseous neutralisation [4]. The bulk decay mechanism is dealing with the transportation of charges through the bulk of the material to ground, while surface decay explains the how charges are transported away along the surface. Lastly, gaseous neutralisation describes how the surface charges are neutralised by free ions in air that could either be by natural or forced air [5].

2.2.1 Bulk conduction

This short will present the charge decay mechanism and its mathematical expression in order to understand the charge's behaviour during the practical lab.

In theory, the number of charges that decrease with time can be derived based on a simple grounded plane with an insulating material on top as in Figure 2.1. The surface charge on the test sample would then create an E-field across the material.

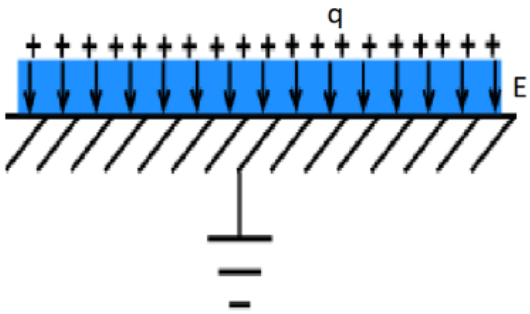

Figure 2.1: Test sample on grounded plane with surface charges

The initial Surface Charge Density σ_0 can be expressed as the total amount of initial charge q_0 across the surface S as in Equation 2.1

$$\sigma_0 = \frac{q_0}{S}. \tag{2.1}$$

By assuming that there are no other conducting element near the test object, one can therefore say that the flux for the surface charges will be directed towards the grounded plane across the test sample, inducing an E-field as following Equation 2.2

$$E = \frac{\sigma}{\varepsilon}. \tag{2.2}$$

The induced E-field will then create a current that wants to pass through the material, which the amount of current is dependent on the resistivity of material hence as seen in Equation 2.3

$$E = J\rho, \tag{2.3}$$

where J is the current density and ρ is the resistivity of the material. The current density J is also affected by the decay mechanism as Equation 2.4

$$J = -\frac{d\sigma}{dt} \tag{2.4}$$

With Equation 2.3 and 2.4, following expression is brought up

$$-\frac{d\sigma}{dt} = \frac{\sigma}{\rho\varepsilon}. \tag{2.5}$$

By solving the Equation 2.5, one can express the surface charge decay as an exponential function, see Equation 2.6

$$\sigma = \sigma_0 e^{\frac{-t}{\tau_0}}. \tag{2.6}$$

The time constant τ_0 is dependent on the material properties,

$$\tau_0 = \rho\varepsilon. \tag{2.7}$$

With the assumption that the surface charge decay is exclusively conducting through the sample as referred to bulk conduction, then Equation 2.6 shall be valid for such case. However, a change of air pressure results in only a reduction of free ions in the atmospheric ambient, hence other decay mechanism shall be taken into consideration when evaluating the de-charging behaviour [6].

2.2.2 Gas neutralisation

Gas neutralisation describes the concept of the surface charges being neutralised by free ions in the air. This phenomenon can also be achieved by placing a grounded element near a positive charged sample, which results in charge transportation through air. The gas neutralisation mechanism depends amount of free ions in the air and the potential of the surface. However to model a general analysis of this behaviour is rather arduous due to many varying factors such as humidity, free ions in air from surrounding elements in the room etc. Studies have also shown that the gas neutralisation or charge decay through air may be a decisive factor for high voltage application and high ohmic value of material, thus resulting in insignificance for lower voltage levels [6].

2.2.3 Surface conduction

Surface conduction can be described as charges moves along the surface towards a grounded point, due to the lower conductivity in comparison to the bulk material and tangential field affecting the direction of travel for the charges [5]. For an uneven charge distribution that is either affected by sample geometry or charging methodology, charges transport along the surface to link. The main factor that affects the degree of surface conduction is from the ambient condition such as humidity and air pollution [4].

2.2.4 Trap energy distribution

For solids, charge trapping inside of the materials can occur due to the materials ability to trap charges inside the bulk during decay. The trap energy distribution can be quantified by finding the energy gap in the solid material as

$$E_0 - E_m = kT \cdot ln(v_0 t) \tag{2.8}$$

where the left hand side represent the energy gap and is influenced by Boltzmann's constant k, the temperature T, frequency of attempted escape v_0 and the time t. The surface potential decay rate is proportional to the de trapping emission current i_d, and the current itself is also proportional to the trap energy density $N(E_m)$ [4]. Therefore the trap energy density can be quantified as following Equation;

$$t\frac{dV}{dt} \propto N(E_m) \tag{2.9}$$

The trap energy distribution of a material based surface potential decay measurements can be illustrated by plotting trap energy density in relation to the energy gap. This distribution is a way to quantify and illustrate the distribution of traps inside the materials.

2.2.5 Conductivity in solids

Conductivity could either be of constant, linear or non linear characteristic. Based on the surface potential decay, the conductivity can be calculated as:

$$\kappa = \varepsilon_r \varepsilon_0 \cdot \frac{\frac{dV}{dt}}{V}, \tag{2.10}$$

where the conductivity κ is dependent on the material permittivity and rate of change of potential divided by the potential at its instant [4]. Thus can different value of conductivity be as results based on different decay rates throughout the time. To find out the degree of field dependent conductivity, the E-field $E(t)$ inside the solid at time t has to be calculated.

2.3 Correlation between simulation and practical experiment

To be able to calculate the surface charge density based on the voltage data measured by the probe, one must know the response characteristic of the measuring probe, which in this case is an electrostatic Kelvin type probe. The basic function of this probe is that it has the same potential as the test sample by connection to a voltage feedback. This mitigates chances of breakdown between probe and test sample [4]. To ensure the accuracy of measurements, the lab setup needs to be simulated and the parasitic capacitance between the probe and grounded needs to be calculated. This is to find out the probe's response function for different measuring position then later on find the relation between measured charge and surface charge density.

For a more complex E-field distribution contributed by the test configuration which both consist of the normal and tangential component. A different approach of obtaining the charge densities may be needed, i.e. By dividing the surface area into smaller sections then later creating a matrix as seen in Figure 2.2, where the row represent position of probe and column position of surface assigned surface charge.

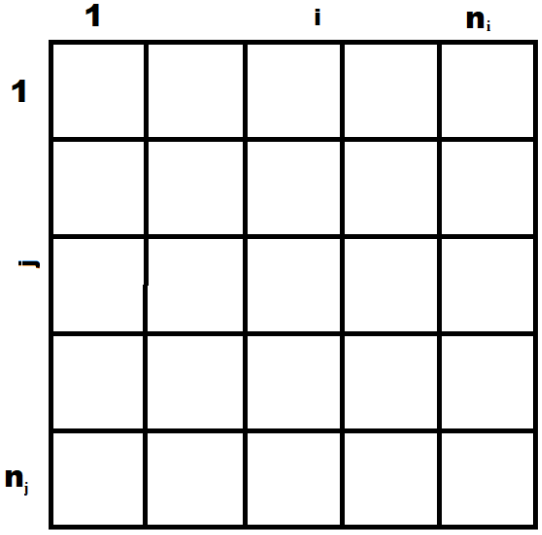

Figure 2.2: Illustration of Φ-matrix with i is position of measured voltage and j is position of unit surface charge density

This section will introduce the principals of obtaining charge densities from a complex test setup by using Φ-matrix. By sectioning the test object's surface area into many section elements, one can implement the Kelvin probes response function for the specific element obtained from simulation [4][7]. The electrostatic probe voltage at a certain position is characterised by following equation 2.11,

$$V_i = \sum_{j=1}^{n} \phi_{i,j}\sigma_j, \tag{2.11}$$

Where ϕ_{ij} is the value of the probes response function at position i,j that is affected by an unit surface charge density σ_j at position j and surface potential V_i at position i. Obtaining the Φ-matrix is done by 3D simulation with exact dimensions to find the exact response characteristic ϕ_{ij} of the probe for each element [7].

After the voltage measurement one can find the correlation between potential and surface charge density at a certain element according to equation 2.12;

$$\left[\overrightarrow{V}\right]_{n,1} = \left[\Phi\right]_{n,n} \left[\overrightarrow{\sigma}\right]_{n,1} \tag{2.12}$$

This allow further evaluation of the amount of surface charge gathered at an element by finding the surface charge density as in equation 2.13

$$\left[\overrightarrow{\sigma}\right] = \left[\Phi\right]^{-1} \left[\overrightarrow{V}\right] \tag{2.13}$$

3
Methodology

This chapter describes the methodology of the executed project, but also the procedure in detail of each part regarding the experiment and simulations. The covered subjects are divided into two main topics, one for the practical experiments and one for simulations. The practical experiments consist of different experiments for example grounded flat gel sample, study of charging behaviour of prototype test cell and lastly charge decay characteristics. The simulations describes how the simulations was conducted in COMSOL multiphysics, i.e. Obtaining the ϕ-matrix to be able to calculate the surface charge density distribution. But also estimation of unmeasurable voltages at certain position inside the test cell. Essentially the methodology of conducting experiments to understand the charging behaviour of the test cell, containing different polymeric materials such as Silicone Rubber (SiR), Glasfiber epoxy (GFR) and silicone gel as presented in previous Figure 1.1.

3.1 Experimentation

The initial part was to set up the laboratory equipment in the facility and familiarize with the setup and the programs. The practical experiments were divided into three different segments, the first consisted of experiments with a grounded flat sample with upper surface open to the ambient while the bottom side was grounded through a layer of aluminium foil. The sample was being held together by a plastic container with the same wall height at the gel, where the charge decay characteristic and electric surface potential was measured. The second part of the experiment were in the constructed test cell with different energizing methods and surface geometries. The energizing methods that was used were corona discharges and pre-energizing. As for the surface geometries, flat gel surface inside the test cell was conducted, but later a rounded surface was also experimented, where there were some hypothesis that the deformations of the gel surface could trigger an electric breakdown.

The third and last part was further investigation into charge decay characteristic, which was conducted as in the experiments using flat gel sample. The goal of the latter mentioned experiments were to review the consistency of the results from flat gel sample experiments, but also to find the materialistic attributes of the gel.

The equipment's and software that were used in the experiment phase consisted of:

- Glassman series FJ ± 60 kV 2mA HVDC source
- Trek model 341B ± 20 kV electrostatic voltmeter connected to Kelvin type

electrostatic probe
- Copley Controls XY robot driven with two stepnet drivers
- DAQ card from national instruments
- Copley control software CME2
- Labview
- Excel for data processing
- COMSOL multiphysics
- Matlab.

The step by step execution of the experiment were as followed,

1. Scan the initial condition of the surface to ensure discharged sample
2. Inserting electrode
3. Turn on voltage source and charge as planned
4. Ground necessary parts
5. Removing electrode
6. Manually moving the robot arm with kelvin probe into start position
7. Run the programmed surface scan program.

As the measurement data were collected through Labview (See Figure 3.2), some post processing method was needed. Depending on the amount of data for each measurements, the goal was to divide the data and to localize the correct voltage for a specific position in the sample. To ensure a good consistency of results as possible, some places in the test cell has been marked to make
Some places in the test cell has been marked to ensure a good consistency of result as possible, for example the configuration of test cell or starting position of probe. But also central position for the energized needle with corona discharges. The programmable XY robot through CME2 (See Figure 3.1), allowed smooth and constant movements of the probe during measurements.

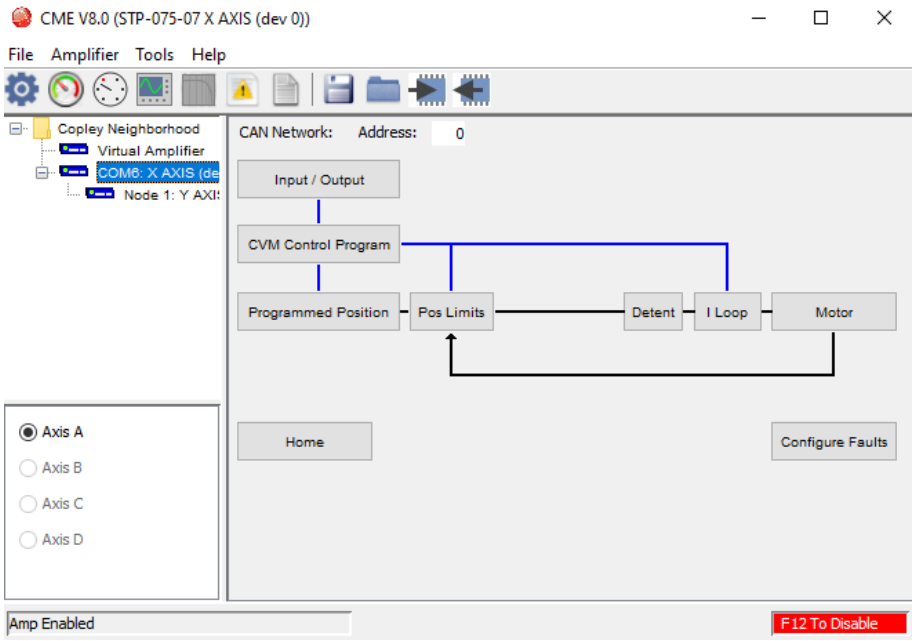

Figure 3.1: Illustration of CME program interface

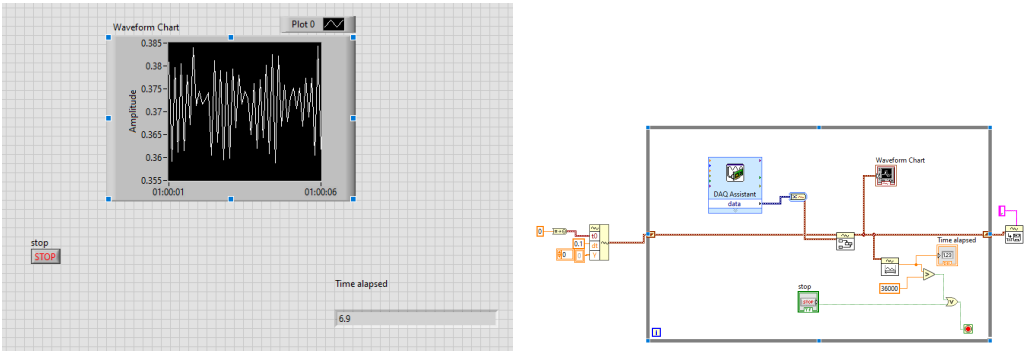

Figure 3.2: Overview of Labview program

3.1.1 Grounded flat sample experiments

In order to interpret the electrical attributes of the gel, some experiments was executed to find the characteristic such as voltage decay characteristics and surface potential distribution. The procedure were executed by applying corona discharges through a needle with different voltage levels above the gel surface as shown in in Figure 3.3.

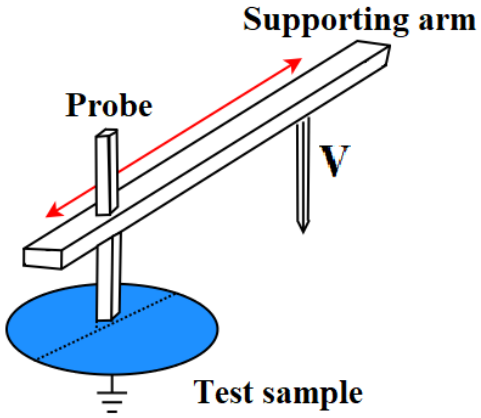

Figure 3.3: Illustration of corona charging setup

After the energizing procedure, the probe was place above and at the center of the sample, with a distance between 2-3 mm. The voltage were then measured and acquired through the DAQ-unit into Labview.

The procedure of charge decay experiments were based on the setup of grounded flat gel sample as illustrated in Figure 3.3. The chosen voltage levels were +10 kV, +7,5 kV and -10 kV, on two identical samples. After discharges of corona, the probe was set manually at above and center of the flat sample to measure the surface potential. The preset settings in Labview were to record one sample every second with 1 Hz sampling time for 36 000 samples, which corresponded to 10 hours. Considered there

was two samples available then the test was conducted with altered samples every test, giving extra time to discharge in case of charge traces left on the sample.

Table 3.1: Overview of charge decay experiment

Overview of amount of repetitive charge decay experiments		
Voltage setting	Sample 1	Sample 2
+10 kV 10 min	3	3
-10 kV 10 min	3	
+7.5 kV 10 min	3	3
-7.5 kV 10 min		

3.1.2 Test cell experiments

For this main laboratory experiment, the robot was reconfigured so that it moves along both the horizontal and vertical lines, this allowed the probe to move along the surface but also being withdrawn from the test cell. Since there was a uniform E-field inside the test cell due to the large sized electrode, the depth was trivial for this measurements.

The test cell was constructed in a way that it would support the gel curing process and rigorous enough to hold when the GFR (Glassfiber) plate were pressed against the gel to form a rounded surface geometry. On the other side of the test cell there were a SiR (Silicone Rubber) plate with another electrode behind. The varying distance ***d*** between the two electric insulation plates could be set to an interval of 30 mm to 150 mm (see Figure 3.4) . The starting distance ***d*** between SiR and GFR plate were set to 130 mm when molding the gel, establishing a flat gel height of 100 mm.

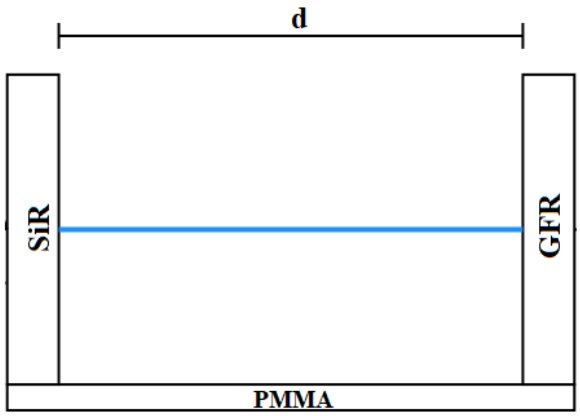

Figure 3.4: Illustration of the test cell

The frame of the test cell was made with PolyMethyl MethAcrylate (PMMA) as seen in Figure 3.5. To be able to energize and ground properly, electrodes were built. For

the SiR plate, a copper electrode was placed at the backside as seen in Figure 3.5 where the cutouts of the PMMA frame was designated for the electrodes. A copper tubing on the electrode was to minimize the chance of unwanted flashover when a higher voltage were used due to sharp edges of the electrode. For the electrode on GFR plate, simply aluminium tape was used due to its sticky properties and easy appliance since the GFR was permanently grounded for this project.

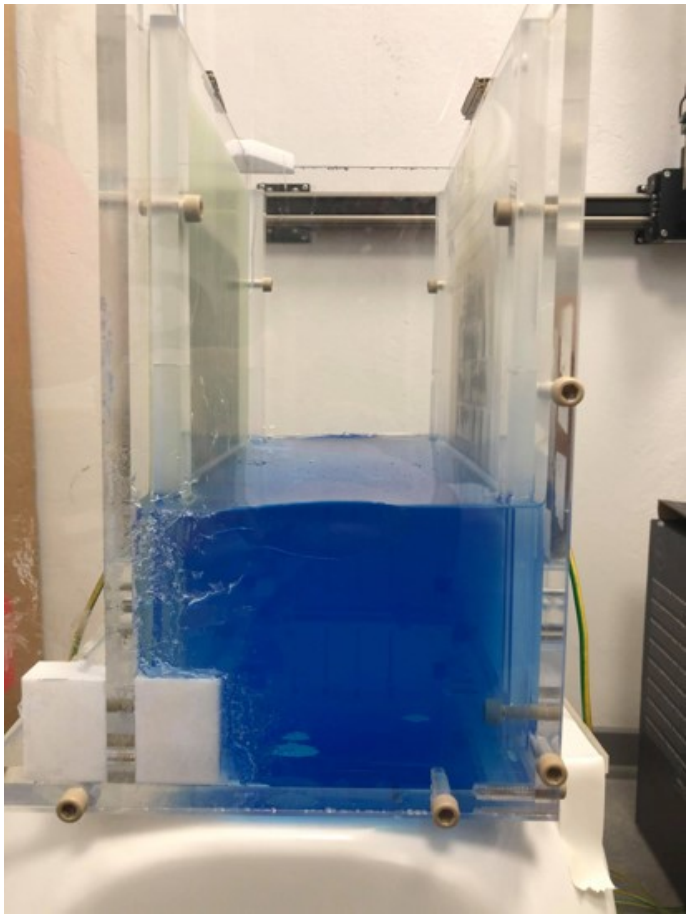

Figure 3.5: Gel filled test cell that was used in the experiments

Two energizing methods were used for the experiment, the first was corona discharges through a needle above the gel surface. The second method was through energizing the HV electrode behind the SiR plate. Depending on which energizing method were used and test cell configuration, different voltage levels and polarities were implemented. Afterwards the probe was placed above the gel surface with the programmed robot to scan the surface potential started at the SiR side and ended at the GFR side. Four measurement scans with 5 minutes intervals were settled to have data for the development of surface potential distribution related with time. However the straps holding the probe to the robot arm resulted to inaccessible measurement position of 10 mm at the furthest end to each plate. Since the size of the probe was 10 mm x 10 mm x 100 mm, only 11 out of 13 equivalent measurement points could be acquired.

The experiment with corona discharges through a needle inside the test cell can be illustrated as in Figure 3.6. The distance between the gel surface and needle were approximately 5 mm, and the predetermined energizing settings were +30 kV, +15 kV and -15 kV for 5 minutes.

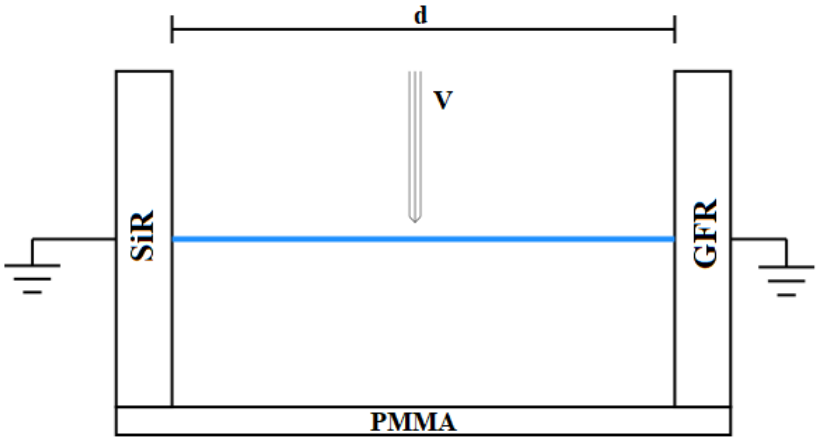

Figure 3.6: Cross section illustration of test cell using corona charge through needle

Other parts of the experiment were conducted by applying high voltage to an electrode behind the SiR plate ensuring a tangential field related to the gel surface, see Figure 3.7. The energizing settings for this section of experiments were set as +60 kV, +30 kV both for 5 minutes and 10 minutes. But also an extra test with -30 kV for 10 minutes were conducted, to investigate the effect of polarity.

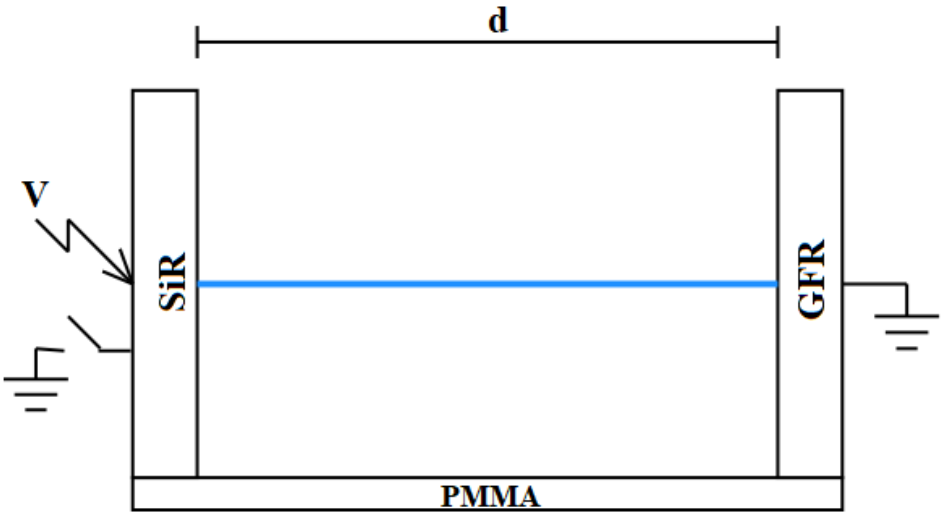

Figure 3.7: Cross section illustration of test cell using energized electrode behind SiR plate

Figure 3.8 represents a rounded gel surface inside the test cell using electrode behind SiR plate to pre-energize. The applied pressure on the supporting bracket holding the GFR plate ensured that the distance ***d*** between SiR and GFR plate were 110 mm, thus resulted in a peak gel height of 115 mm. This configuration was brought up mainly for suspicion that the bumped surface geometry would cause electrical failure when exceeding a certain voltage level. The measurable position closest to the SiR plate in this configuration was only measured due to insufficient programming of the robot.

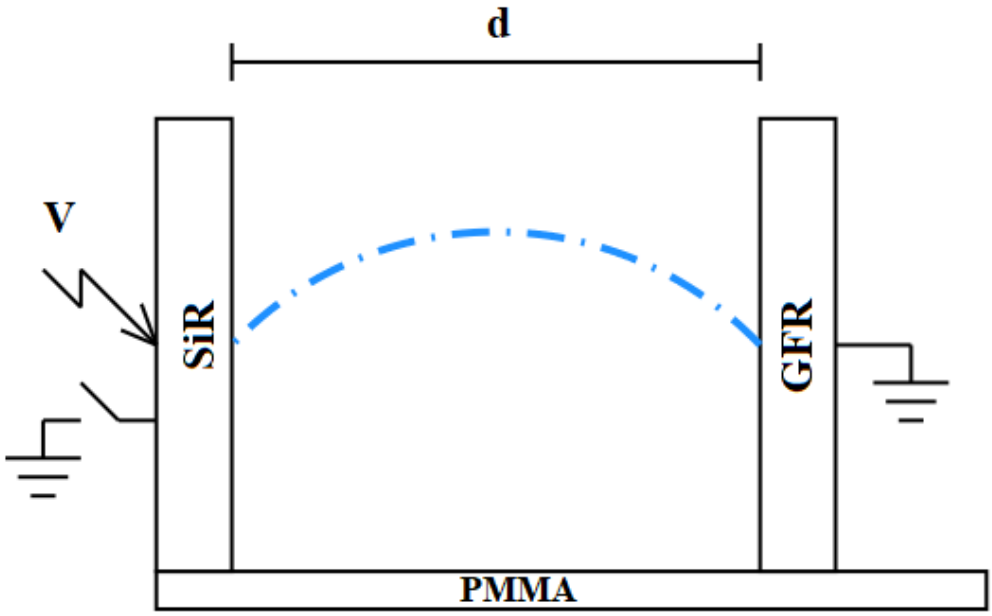

Figure 3.8: Cross section illustration of test cell with rounded gel surface using energized electrode behind SiR plate

To have an easier overview of the conducted experiment and its content, See Table 3.2. As one noticed, majority of experiments in the table were not conducted due to hypothetically no relevant results could be collected.

Table 3.2: Overview of experiments in test cell

Numbers of repetitive experiments conducted in test cell				
Surface Geometry	Flat	Rounded	flat	Rounded
Charge Setting	Corona discharges through needle		Energizing behind SiR plate	
+15 kV 5 min	3			
-15 kV 5 min	3			
+30 kV 5 min	3		3	
+30 kV 10 min			3	3
-30 kV 10 min			3	3
+60 kV 5 min			3	
+60 kV 10 min			3	

3.2 COMSOL simulations

This section comprehends the content of the project regarding simulation in COMSOL. Simulation were needed to be made in order to find the responce characteristic of the measurement probe. Since in general for every experiment different surrounding elements may contribute to stray capacitance that might effect the probe. Therefore simulations with test cell were simulated to find the correct response function of the probe for this specific experiment.

3.2.1 Obtaining ϕ-matrix

The step by step methodology behind the simulation phase, before evaluating the data concerning the surface charge density distribution, can be found in the below section. The intention of this simulation was to fully understand the response function of the measurement probe, by constructing a corresponding model in COMSOL. The simulation was conducted in COMSOL multiphysics by constructing the test cell with the gel consisted of 13 domains with 10 mm thickness, making a total thickness of 130 mm as in the physical test cell. On each end of the gel, SiR and GFR plates where placed with a thickness of 7 mm. A rectangular cuboid that was supposed to mimic the probe with dimension of 10 mm X 10 mm X 100 mm. Lastly a large enough air boundary surrounded the test cell in order for the simulation to work, as seen in Figure 3.9.

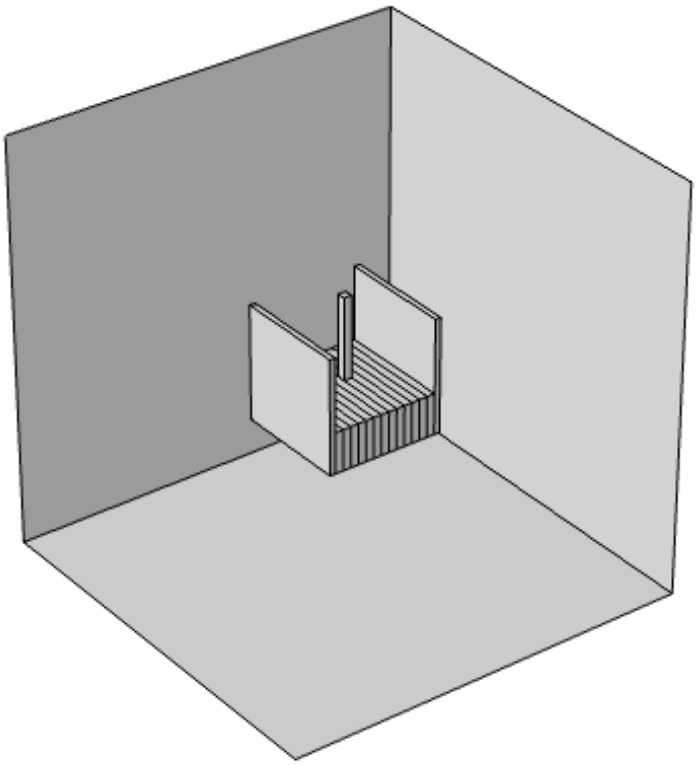

Figure 3.9: Overview of 3D modelled test cell.

As for the assigned relative permittivity for the geometries in the model can be found in following table 3.3. The assigned material properties for the Kelvin probe was based on COMSOL's database for Iron.

Table 3.3: Material properties assigned to the constructed geometry domains[2]

Material	**Relative permittivity** ε_r
Air	1
POWERSIL	2,5
SiR	3
GFR	5

The used physics for this simulation was ***Electrostatics (es)*** which consisted of assigned grounding on the outer side of the SiR and GFR plates (See Figure 3.10).

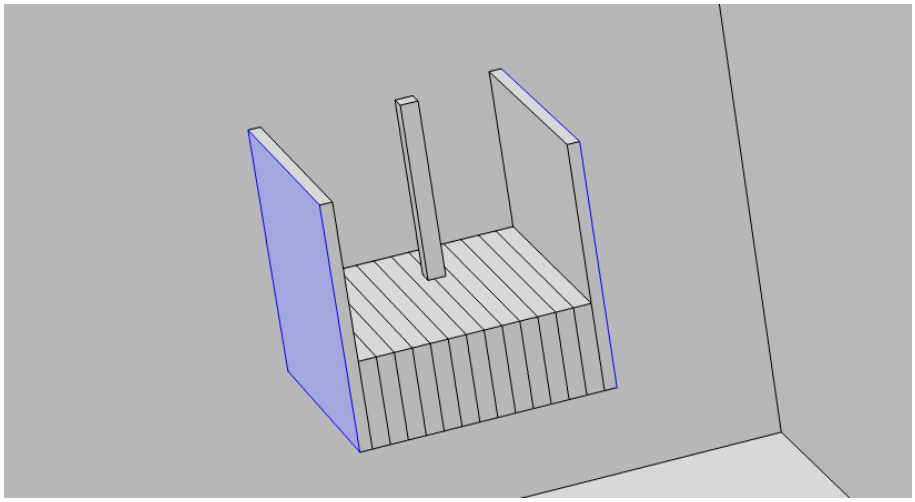

Figure 3.10: Assigned grounding on test cell.

For physics regarded the probe was only electric potential with variable "vprobe", which initial value were appointed to 0V (see Figure 3.11).

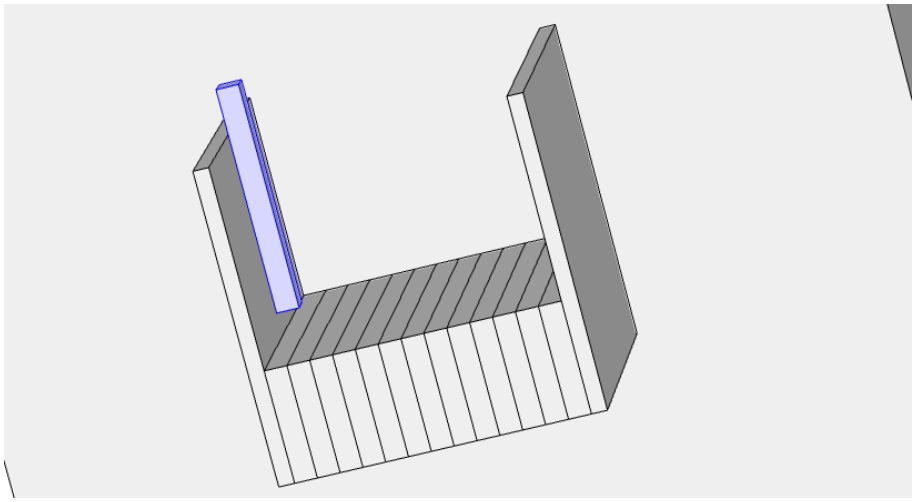

Figure 3.11: Assigned potential to probe domain.

To be able to generate the ϕ-matrix, one had to assign $1\mu C/m^2$ of surface charge into one of the gel elements, while the other elements are kept at zero charge as seen in Figure 3.12. For this scenario there was 13 elements of gel, therefore gave a total size of the ϕ-matrix of 13x13 elements. Each row should represent the position of the probe over each gel domain, whilst each column represented the position of applied $1\mu C/m^2$ surface charge.

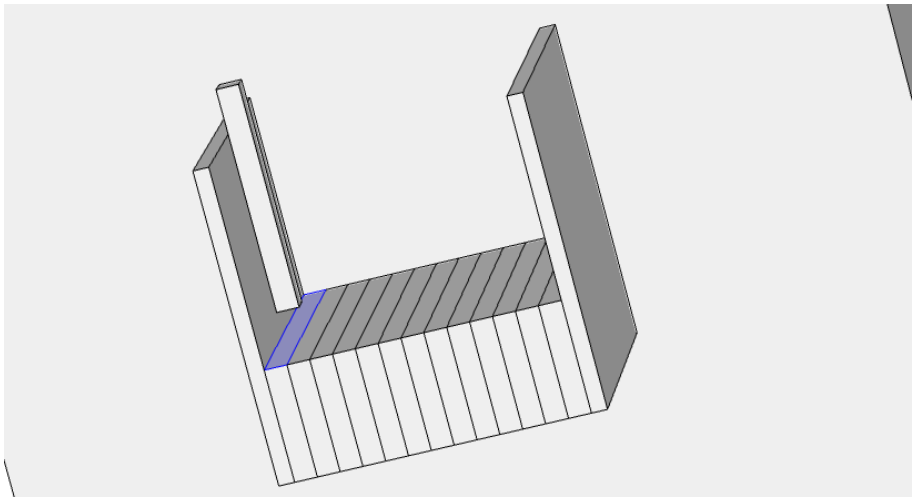

Figure 3.12: Assigned charge in the first gel domain.

To be able to find the correct value of each element in the ϕ-matrix, some implementation in the COMSOL solver had to been made. The first was to implement a parametric sweep for the variable *vprobe* with initial value 0 V and final value of 1000V with each step raising 50 V. This resulted in a linear voltage profile of the probe which was crucial in order to find the correct ϕ-matrix value. The linear voltage profile was later plotted into the same graph as the electric surface potential of the gel beneath the kelvin probe as seen in Figure 3.13. The blue line represented the linear voltage function of the kelvin probe and the green line shows the electric surface potential as stated above. The intersection of these two lines was the

value for one specific element in the matrix. To fully fill the ϕ-matrix, repetitive simulation with different position of charge and probe had to been made.

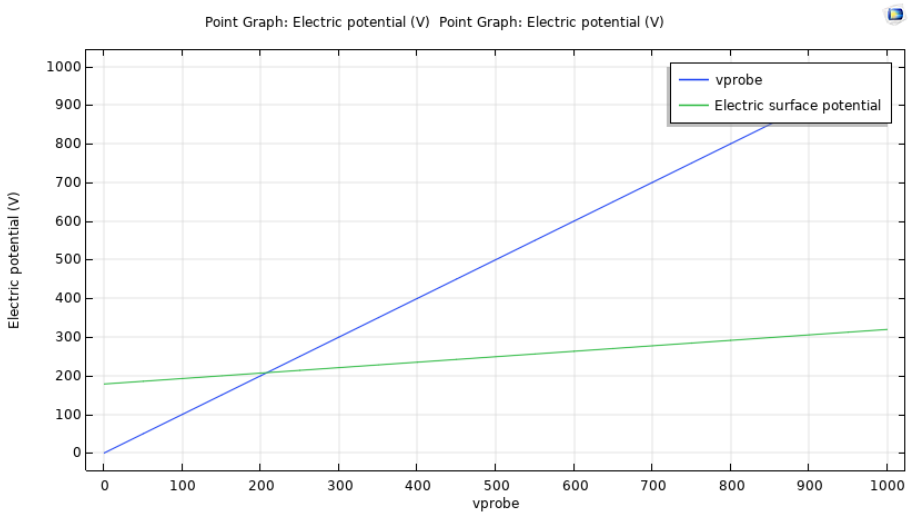

Figure 3.13: Graph showing the first element in the ϕ-matrix.

3.2.2 Simulation of electric surface potential

11 out of 13 positions in the test cell were reachable for the probe, however the furthest position at each end was not reachable due to physical constraint of the supporting arm holding the probe. By having this restriction, one had to find a way of estimating the voltage of both positions. One approach of estimating the voltage was simulation through COMSOL by implementing the computational test cell as described previous, however with a few modifications. One of the modifications was applying the measured surface voltage distribution instead of surface charge, into the 11 domains and afterwards the total surface potential distribution could be plotted in COMSOL as in Figure 3.14.

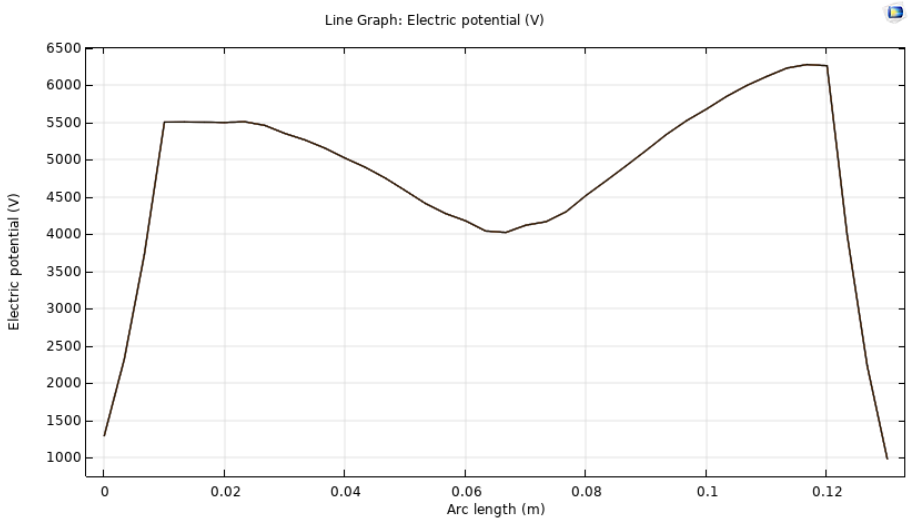

Figure 3.14: Simulated electric surface potential distribution based on +30 kV Corona Discharges through needle

However based on Figure 3.14 the slope at each end is very steep, therefore two cut point 3D was implemented at the center of both outer domains as seen in Figure 3.15. With the help of those cut points, one was able to find a concrete voltage value of both domains as seen in Figure 3.16.

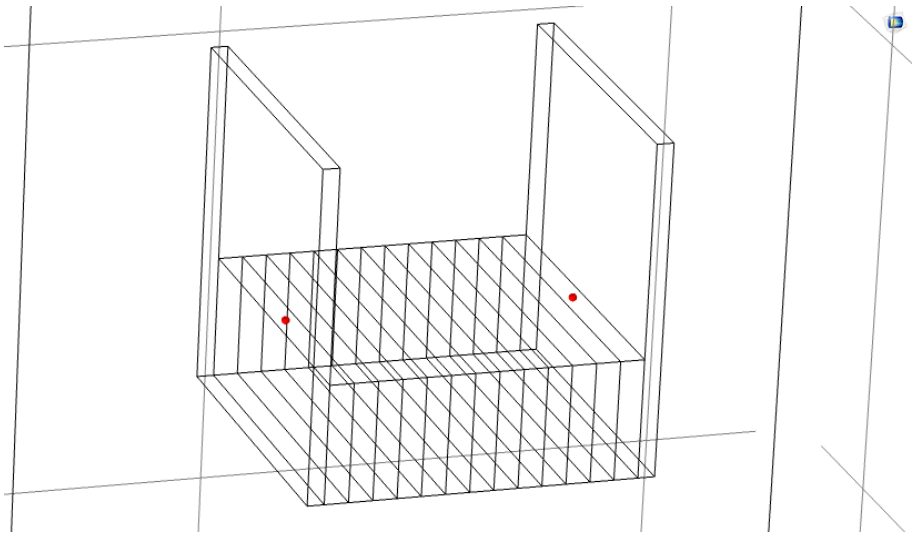

Figure 3.15: Two cut point 3D implemented into the test cell

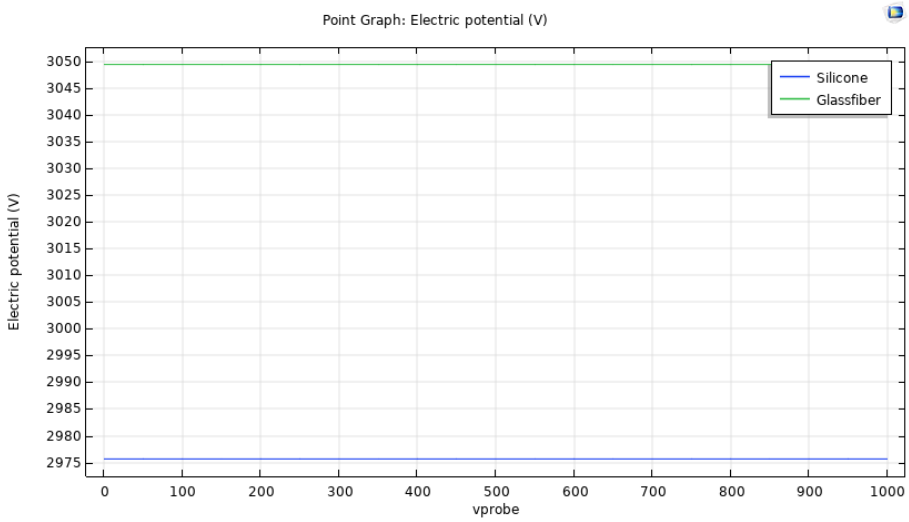

Figure 3.16: Simulated voltage level at the furthest domain in the test cell

4

Results and Discussion

This chapter will present the results from the conducted experiments based on the described laboratory implementation. The structure of display will be matched as previous, starting with experiments on a flat gel sample in a plastic container with its upper surface open to ambient air while the bottom surface is grounded through an aluminium foil. Followed up with experiment implementing the test cell with different charging settings and surface geometries. Based on these two experiments data, information can be interpreted for research purposes and further development of the dry application HV cable termination.

4.1 Experiments on flat material sample

On the this study of the gelatinous insulation material where the surface potential distribution and decay were of primarily interests. The idea behind this study was to have an understanding of the charge dynamics of the material when exposed to corona charging. Different voltage levels where used in this study consisting of +5 kV, +7.5 kV and +10 kV.

4.1.1 Surface potential distribution

As shown in Figure 4.1, 4.2 and 4.3, the potential distribution was more or less symmetric. Looking at Figure 4.1, it is noticeable that the shape of surface potential distribution did not change significantly during decay . The highest voltage amplitude can be seen at the center of the sample, above which the charging needle was positioned.

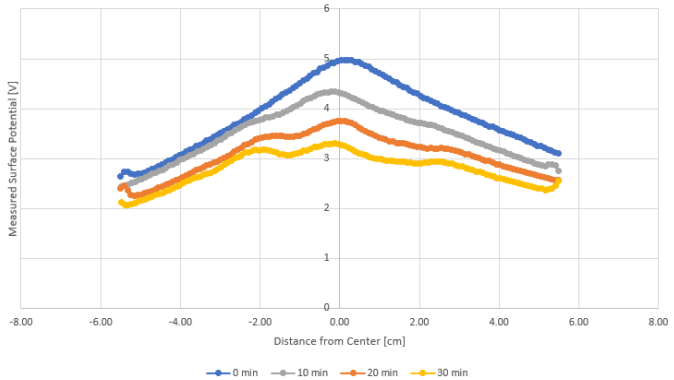

Figure 4.1: +5 kV corona charge on flat uniform sample

In Figure 4.2 illustrates the potential distribution based on the acquired data from the experiment. It is noticeable that there were some data errors at the far edges of both sides. This is due to the Kelvin probe measuring above or to near the container of diameter 100 mm, hence the large drop in potential. However as for the surface potential distribution it follows the same trend as in previous experiment of +5kv charging.

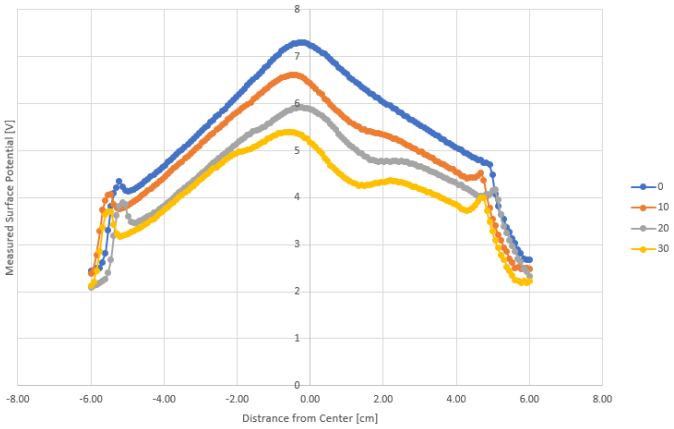

Figure 4.2: +7,5 kV corona charge on flat uniform sample

In Figure 4.3 illustrates the measured data acquired from an experiment of +10 kV corona discharging at flat gel sample. However looking at the blue curve 0 min, one can notice that the amplitude exceeds 10 kV at the center, which was due to an error in the voltage source when getting heated. One can also notice similar noises at both edges as previous cases, which could be excluded when post processing the data as in 4.1.

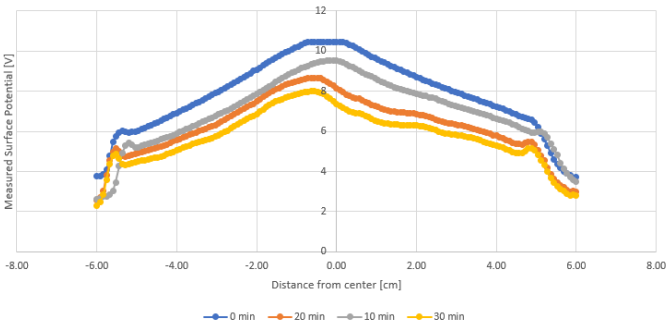

Figure 4.3: +10 kV corona charge on flat uniform sample

In general the surface potential is more or less symmetric directly after the charging procedure. However one can see that the potential distribution with time is getting more distorted which can be seen in Figure 4.1, 4.2, 4.3 as the grey and yellow curve. This distortion is possibly caused due to creases in the aluminium foil when inserting inside the container, resulting in unevenness. The unevenness was calculated to a maximum error of 20% in relation to the gel.

However, the results may be off by some margin of error depending on the method after applied corona charges since there are two measuring procedure to choose between,

1. Turn off voltage source before removing away the needle, later insert Kelvin probe to desired position.
2. Removing the needle away before turning off the voltage source, later inserting the Kelvin probe to desired position.

The first method allows no further charging when moving away the needle, which results in a more symmetric charge distribution along the surface. The drawback of this method is that when the voltage source is turned off, the needle becomes a grounded point and some charge neutralisation through gas occurs.
The second methods allows fully charged sample before inserting the probe which is beneficial for potential decay measurement, since the surface charge distribution is not in interest for such measurement hence, the measuring position is at the direct center of the sample. The effects on results by having the probe near the sample for a longer time has been shown to have no larger significance due to its field zeroing technique [8]. Nonetheless this zeroing technique might be an issue in later measurements which will be discussed.

4.1.2 Potential decay

For the potential decay of the sample, one can notice that the rate of decay in the insulating material is exponential and it takes about 8 hours for the potential to fully decay for all three cases of different voltage levels. It is also notable that the curves cross over each other, due to field dependency of conductivity in the material that could be related to Equation 2.2 [9]. The starting voltage of each curve in Figure 4.4 did not reach up to the same voltage as the voltage source itself, however this could be achieved with a matter of charging time, as previous test could attain the same voltage level, see Figure 4.3.

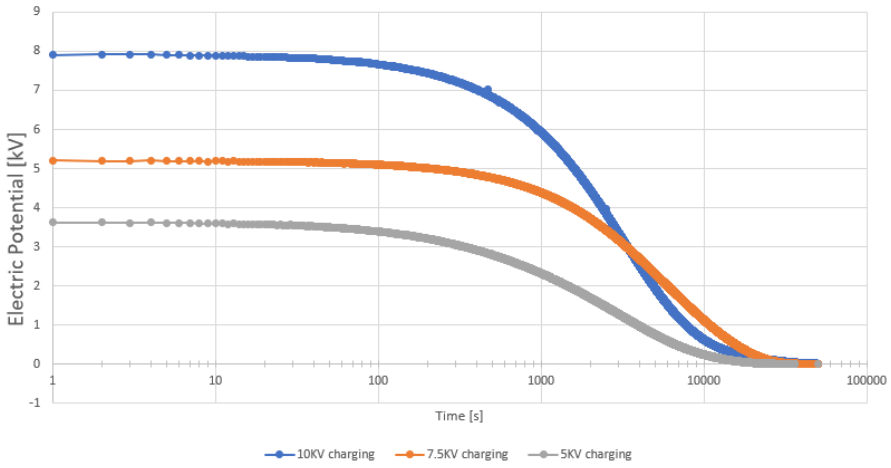

Figure 4.4: Charge decay measurement on flat uniform sample

Since there were two samples that were available to conduct the test in, one had to assure that the samples would give a consistent result as seen in Figure 4.5, where the curve could be observed to more or less identical. The total sampling time were set to 10 hours and by then the sample were more or less fully discharged. However besides bulk conduction, only natural gas neutralization were implemented, one could expect a slower decay rate for lower potentials[8].

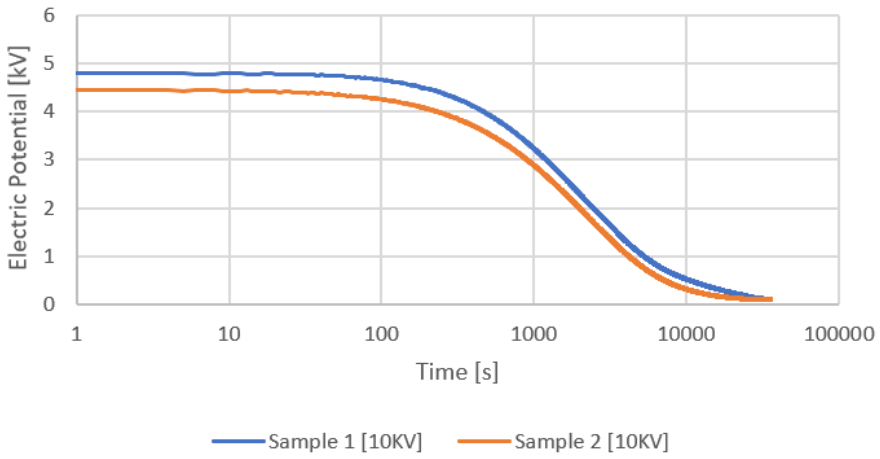

Figure 4.5: Charge decay characteristics comparison between two samples

The first experiments that was mentioned above gave an indication that the gel would be electric field dependent and as the continuation of the experiments that were later conducted, it showed the same charge decay characteristic. As discussed in earlier one could observed the two curves crossing even for the later tests, therefore the field dependent characteristics could be once detected [9]. However, further investigation upon the characteristic can be made since individual charge decay mechanism were not in trial during this experiment.

The significance of charging polarity could be observed in Figure 4.6, whereas it had no greater significance [8]. The curves were approximately identical with few deviation at the beginning and the end. However since the charge decay experiment were conducted in parallel with the test cell experiment, some corona discharges might have happen before the decay experiment, thus enhancing the decay mechanism.

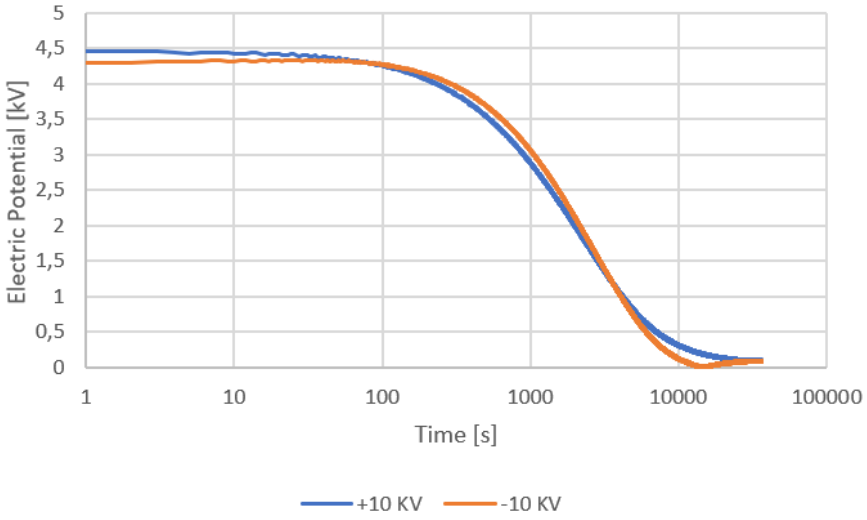

Figure 4.6: Electrical potential decay comparison for two voltage polarities

According to the data sheet of insulation gel, it has a relative permittivity of 2.5 and conductivity of $10^{-14}S/m$[2]. The conductivity of air has a range of $10^{-15}S/m$ to $10^{-9}S/m$, however this value is geographically dependent [10][11]. For standard comparison one can assume an air conductivity of $10^{-15}S/m$, which means that the gel is more conductive than air. Related to this project, one may assume that the charge through bulk decay mechanism is more dominant than gas neutralization.

4.1.3 Material characterisation

Based on the data values collected from experiments on flat gel sample, the characterisation of the material could be analysed. Implementation of Equation 2.10 gave an mapping of the conductivity with respect to the internal electric field as seen in Figure 4.7,

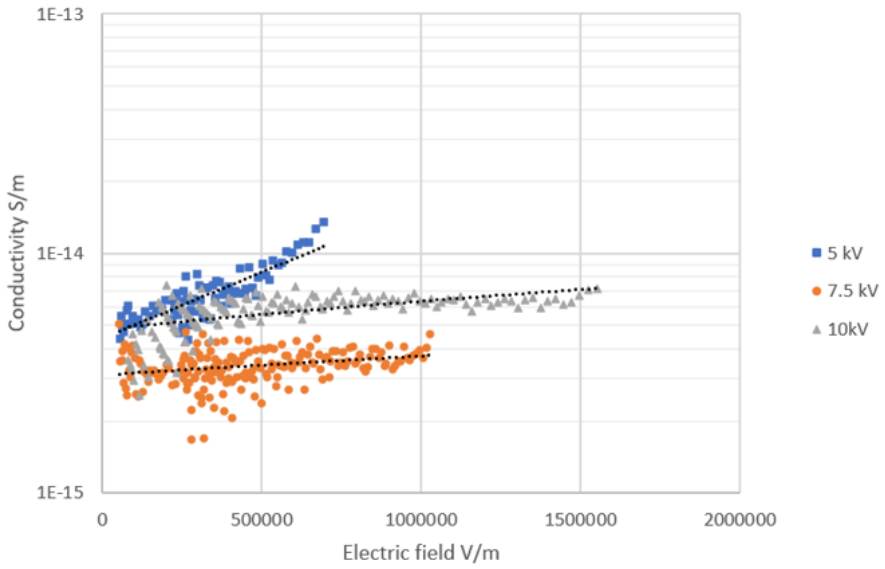

Figure 4.7: Calculated conductivity in relation to internal E-field.

As noted in the figure above, one can see the exponential field dependency of the conductivity, with the a cluster of data points around $10^{-14} S/m$ which is in range according to the data sheet [2]. The influence of field dependent conductivity affects the charge decay of the gel, which could determine the performance of the cable termination. However for this case with a small fluctuation of conductivity around the data sheet value, no larger impact of the performance would be present. Taken the gel into comparison with the other polymeric material inside the termination, the conductivity is more or less the same [12]. However, the values are generalised and many different version of silicone rubber and glass fiber epoxy are available which results in a further measurements of the actual material used for the cable termination is needed.

Besides calculation of conductivity, the trap energy distribution was also calculated. Since the gel is considered as a solid material, investigation upon the charge traps inside the bulk was executed. As seen in the Figure 4.8 the trap energy distribution was calculated with the Equation 2.9 and 2.8, the peak trap energies was located approximately around the same energy gap interval at the higher end of 0.8 eV. The quantity tdv/dt , which is proportional to trap density has a peak of 3000 at 10 kV charging". This peak value reduces to 2000 and 1000 when charging voltage decreases to 7.5 kV and 5 kV respectively. This indicate that there are some traps inside the gel that get activated only at high fielded conditions.

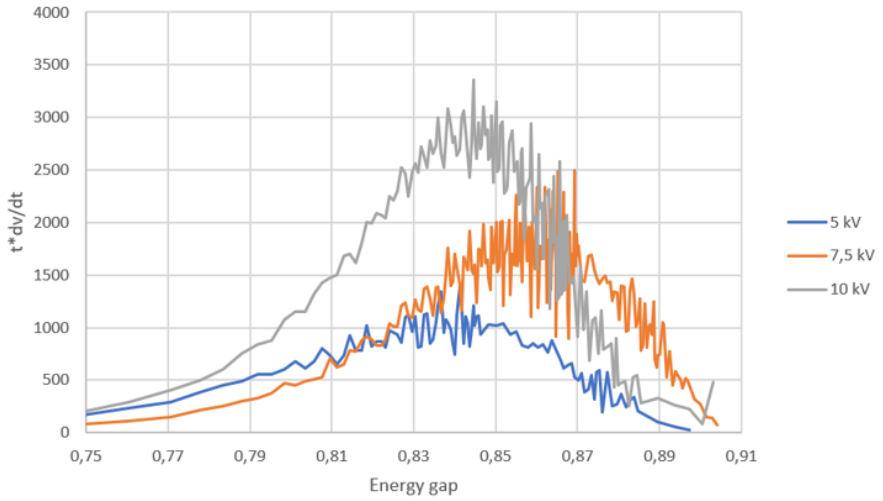

Figure 4.8: Trap energy distribution in insulation gel

4.2 Corona charging inside test cell

The first section of experiment in the test cell was using an energized needle in the center of the of test cell with a distance about 1cm above surface of the gelatinous insulating material. The anticipation of this conducted test was to understand the role and effects of supporting insulating materials, in this case; silicone rubber (SiR) and glass fiber (GFR). For this particular test, three different voltage levels were used, +30 kV, +15 kV and -15 kV. The charging time were set to 5 minutes.

4.2.1 Surface Potential and charge density distribution

First result to be presented is the measurements that were gathered from the +30 kV experiment. Figure 4.9 shows the surface potential distribution with 11 measured point followed with 1 simulated point at each end, resulting in a total array size of 13 elements. The starting potential at the furthest measured ends had approximately the same amplitude, this margin of error could be due to the fact that the needle is placed by hand into the test cell with approximation to the center. When elapsed time taken into consideration, the potential decayed much faster at the silicone rubber side which can be found in element -5 cm in Figure 4.9, in comparison to the glass fiber side at element +5 cm.

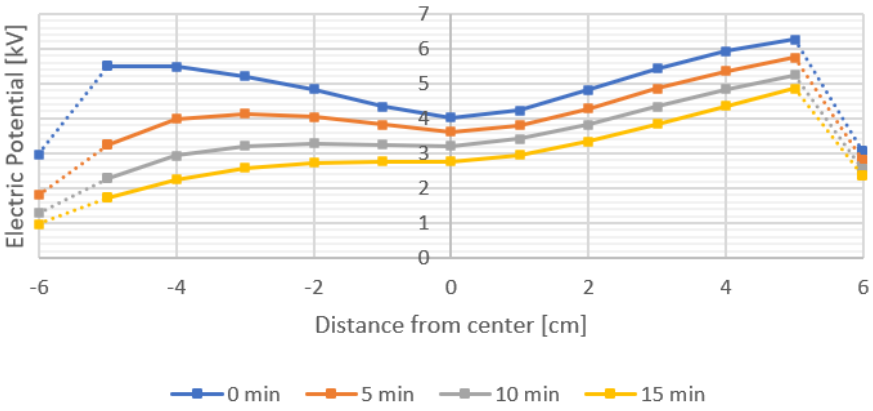

Figure 4.9: Surface potential distribution from tangential electric field, Corona charging +30 kV

The calculated surface charge density distribution that was based on the surface potential distribution in Figure 4.9 can be found in Figure 4.10. As one can see the surface charge density could be reasonably related to the voltage distribution. Based on this results one can understand the effects of supporting material in the whole application.

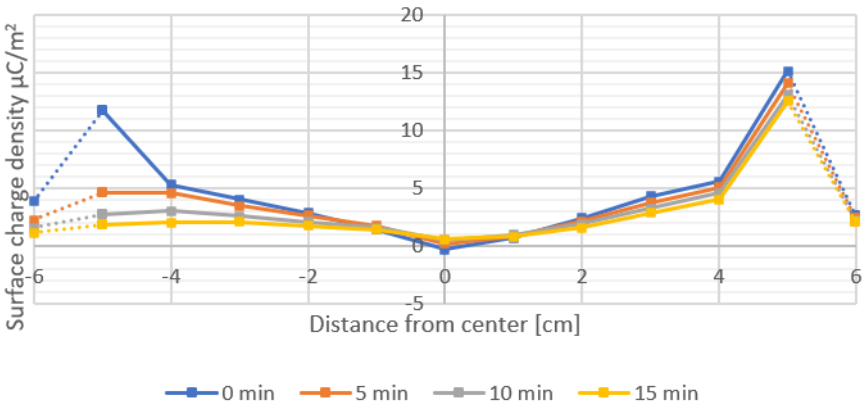

Figure 4.10: Surface charge density distribution from tangential electric field, Corona charging +30 kV

The blue curve "0 min" in Figure 4.10 was then taken into calculation of E-field distribution for both along the surface and through the bulk. Figure 4.11 represented the E-field where x component is along the surface while z component is through the bulk. Looking at the surface charge density distribution in Figure 4.10, there were one peak at each end of the test cell. However this peak contributes to different E-field, for instance at the SiR side there was a E-field cancellation at the same time there was an enhancement of E-field near the GFR side. With a distance of 130 mm between the polymer plates and +30 kV needle at the center results in an average E-field of 0.46 kV/mm. The peak amplitude of surface E-field at SiR and GFR sides was around -0.25 kV/mm respectively 0.35 kV/mm, which was not enough to trigger a corona discharge with breakdown criterion of 3 kV/mm. As for the bulk

the E-field at furthest end were more or less 0, which bulk decay can almost me neglected at those position. However going a bit towards the middle about 10 mm, there was a significance concentration of E-field. This was due to the high surface charge density at those position.

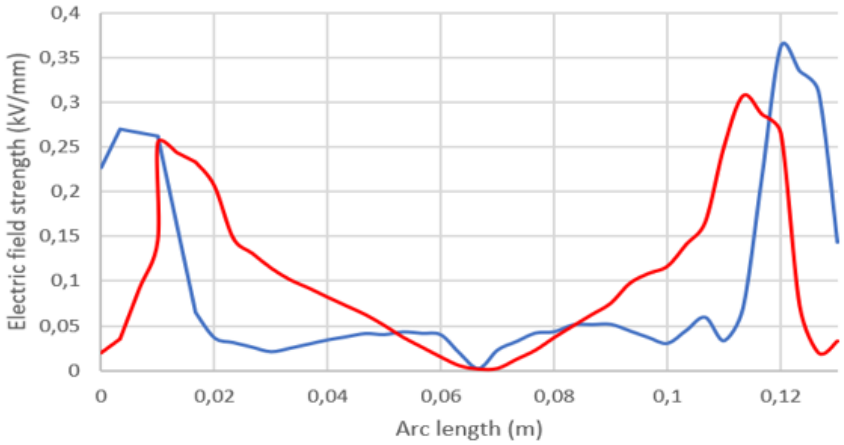

Figure 4.11: E-field calculation based on +30 kV 5min needle charging.

4.2.2 Potential decay comparison

When the data from Figure 4.9 was reformulated, one could arrange and compare the potential decay rate at each furthest measured point as seen in Figure 4.12. As stated above, the deviation of voltage amplitude at time 0 could be due to off-center placement of the needle or the fact that the conductivity of both material are different. The Figure 4.12 evidently shows the rate of decay near each supporting material. The latter statement could play a large role into further development of the real application.

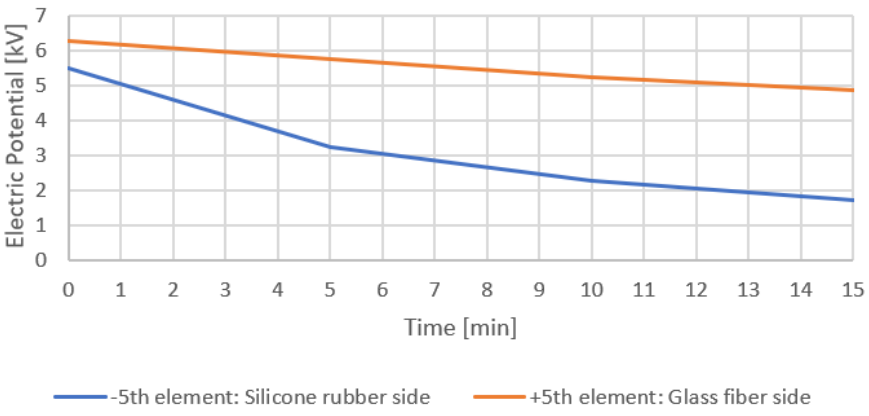

Figure 4.12: Surface Potential decay at each furthest measured point from tangential electric field, Corona charging +30 kV

4.2.3 Effects of polarity

The second and third charging condition consisted of +15 kV and -15 kV which is supposed to give an indication of the polarity effects in the test setup. Following Figure 4.13 shows the potential distribution from a charging level of +15 kV, which showed similar distribution as the previous case of +30 kV.

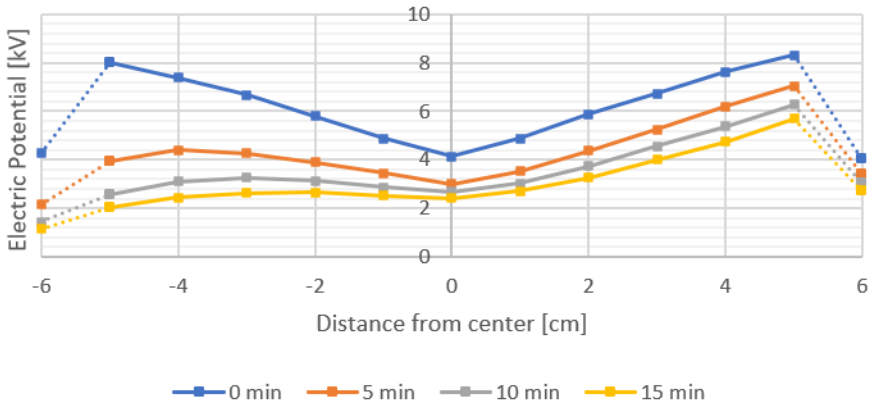

Figure 4.13: Surface potential distribution from tangential electric field, Corona charging +15 kV

The related surface charge density distribution in Figure 4.14 follows the same trend as in previous cases.

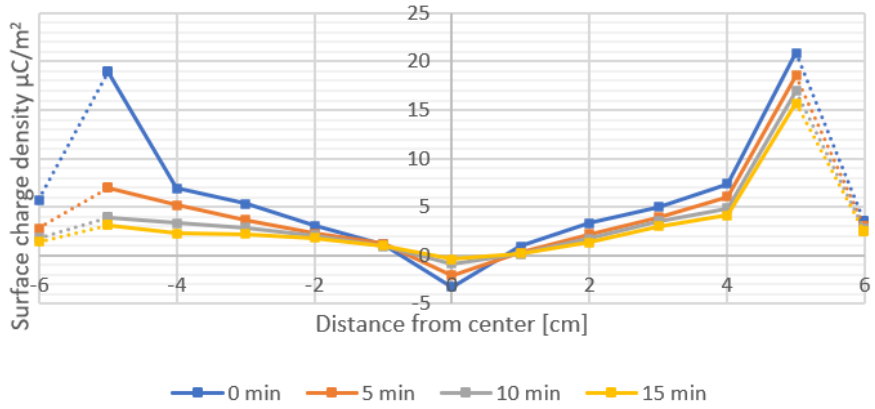

Figure 4.14: Surface charge density distribution from tangential electric field, Corona charging +15 kV

As for the negative polarity of 15 kV, the results seen in Figure 4.15 has been presented as absolute value for easier comparison with the preceding results.

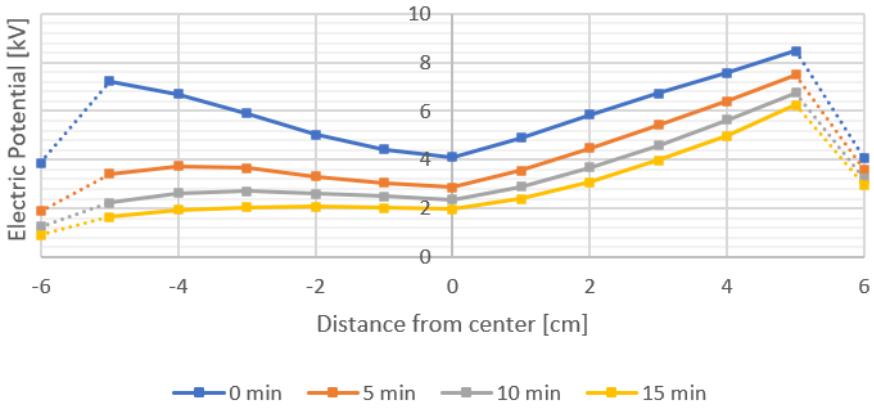

Figure 4.15: Surface potential distribution from tangential electric field, Corona charging -15 kV

The calculated surface charge density distribution as seen in Figure 4.16 will be used into evaluation the effects of polarity.

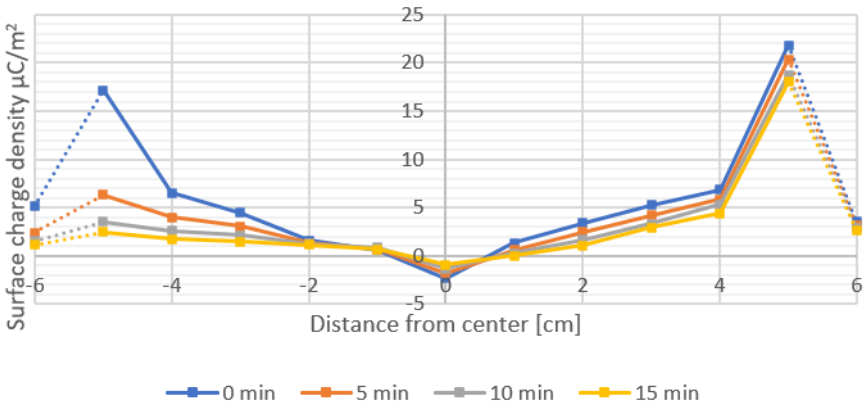

Figure 4.16: Surface charge density distribution from tangential electric field, Corona charging -15 kV

When the data in -5th respectively +5th element was taken into comparison, following Figure 4.17 can be engendered. The squared breakpoints represent the glass fiber side and the rounded breakpoints for the silicone rubber side. As stated in previous statement, the potential near the silicone rubber was discharging at a faster pace in comparison to glass fiber side. however no matter of polarity, the decay had same rate near both materials. Since the electric field between the needle and grounded electrode had the normal component, most of the decay was through the bulk of each material as described in Chapter 2.2.1 [8]. However related to the gel the electric field had a tangential component and thus may have resulted in surface conduction in the gel [4][5].

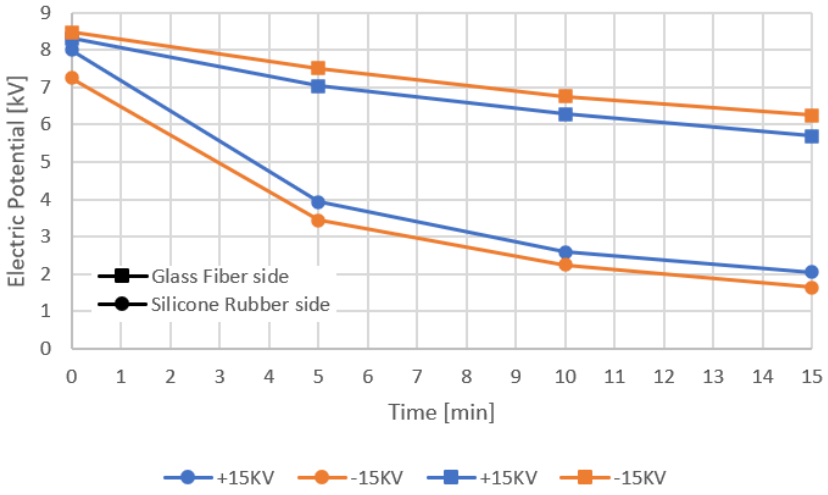

Figure 4.17: Comparison between charging polarity at each end of test cell

4.3 Energized test cell using HV electrode

This section will comprehend the experiments results from using the HV electrode beside the test cell, namely the electrode located behind the silicone rubber plate. This setups applied a tangential field on the gelatinous insulation material, and the speculation behind this was to find the surface potential and charge density distribution.

In Figure 4.18 one can see that after 10 minutes the surface potential distribution was more center focused in comparison with min 0, which the larger amount of potential is near the left region where the energized electrode is located. The electric potential close to the SiR could be measured up to 4 kV while as for the GFR the potential were only 2 kV.

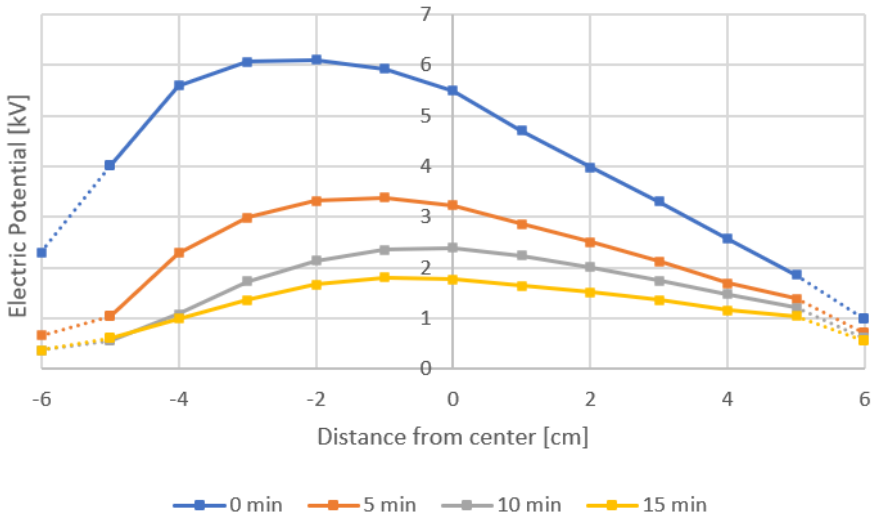

Figure 4.18: Surface potential distribution from tangential electric field, Energized electrode, +60 kV for 10 min

As for the calculated surface charge density that can be seen in Figure 4.19, at the orange curve 5 min, at -5th element there was a negative charge density even though the voltage at that position could be measured. It is uncertain whether this point could be interpreted as negative charge or a pure error in the model. However, in general the surface charge density distribution is more dominant on the left side but with time the majority of charges are still at the center. Even after 15 minutes on can still expect some charge at the center of the surface with an amplitude of 1-2 $\mu C/m^2$. Since there are no grounded elements near the center or beneath the gel, most of the charge decay mechanism will either be through surface conduction or gas neutralization.

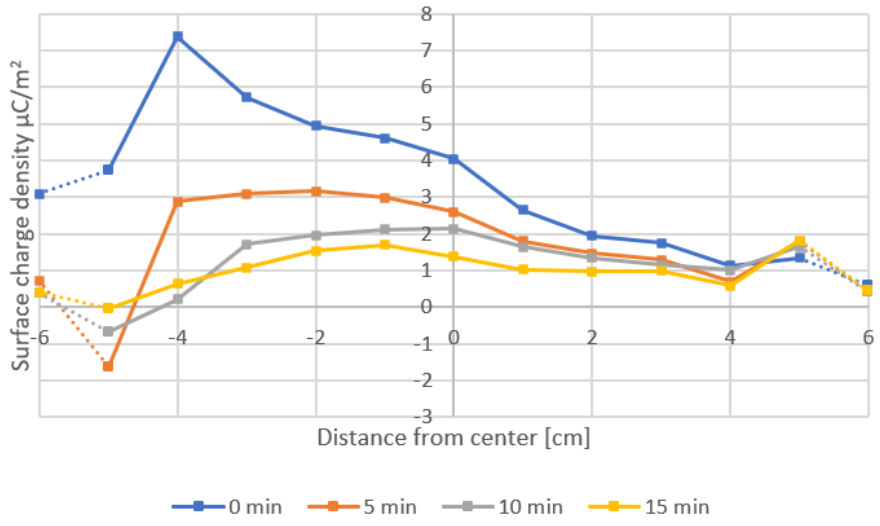

Figure 4.19: Surface charge density distribution from tangential electric field, Energized electrode, +60 kV for 10 min

When the surface charge density distribution was implemented in in the test cell simulation, one could plot the E-field distribution as seen in Figure 4.20. The blue curve represent the x component which is along the gel surface while the red curve represent the z component which goes inside the bulk of gel. It is noticeable that there was a field cancellation at the left region because of locally higher surface charge density. When taken the E-field magnitude at each ends into comparison, there is a difference in magnitude which explains the fact that the surface charge density distribution is getting more center focused. As the first experiments using flat gel sample, the charge decay rate of the gel is field dependent, hence the faster charge decay at the SiR region. For the z component the magnitude of E-field at each end is almost zero which presumably result no bulk conduction at these regions. However going more towards the middle, there is an E-field going through the bulk which one can expect a limited bulk conduction. However it is difficult to distinguish and separate how much of each charge decay mechanism is working the most in this setup. In Figure 4.20 for the blue curve x component at 0.1 m, one can see a field enhancement in that area. This field enhancement could lead to initiation of breakdown in that area, as parallel studies has shown. Although it is an indication of local field enhancement near the SiR plate, it is not for sure granted that the result might be reliable due to the fact that it was not possible to measure that area with the probe. Nor is were any measurement taken on the SiR plate that also might has influenced the field distribution in the triple junction.

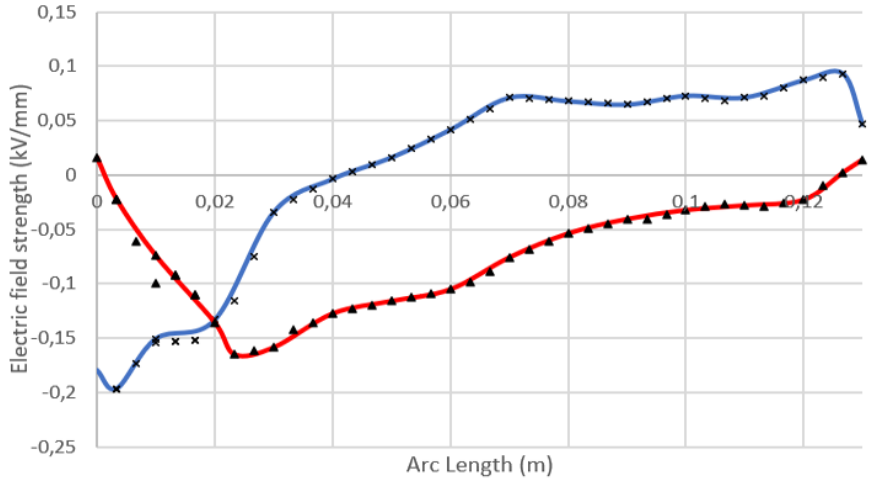

Figure 4.20: Calculated E-field at min 0 in the gel based on surface charge density from 60 kV 10min energizing

Surface potential and charge density distribution for every charging level was taken into comparison. In Figure 4.21, the surface potential distribution for every voltage level at time 0 min was presented in one plot. The curves are divided into two different colors, the blue color with various shades represent 60 kV charging level and the amber colors represented 30 kV. Essentially, the majority of potential are focused at the left region, however for the lower voltage one can notice a more even distribution along the gel surface in contrary to the higher voltage level of 60 kV. In Figure 4.22 the different surface charge density distribution were put into

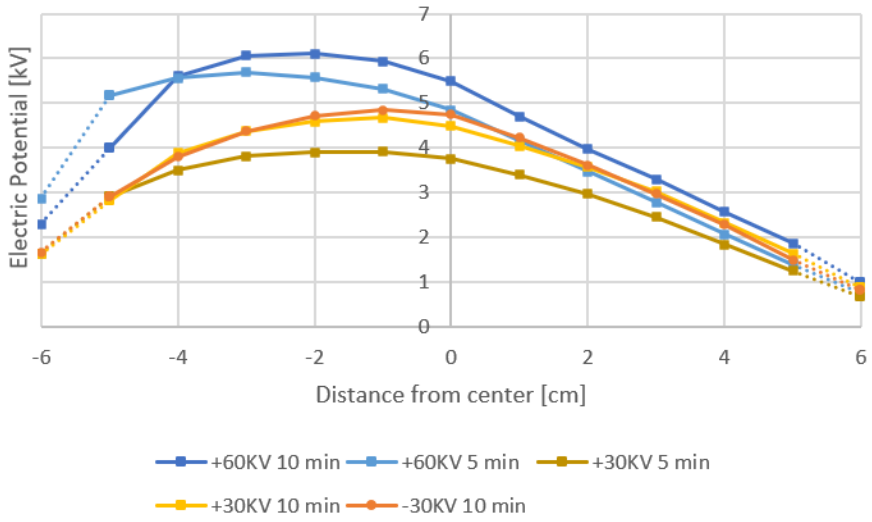

Figure 4.21: Surface potential distribution comparison for different voltage levels

comparison. It was noticeable that there was not much of a irregularity except both of the blue curves at -4th and -5th element, where the density was calculated to a higher value. As for the 30 kV levels, looking at the amber curves, there are not distinctive peak of charge density in comparison with the 60 kV cases. Therefore can one expect a concentrated charge density near the SiR for a higher voltage.

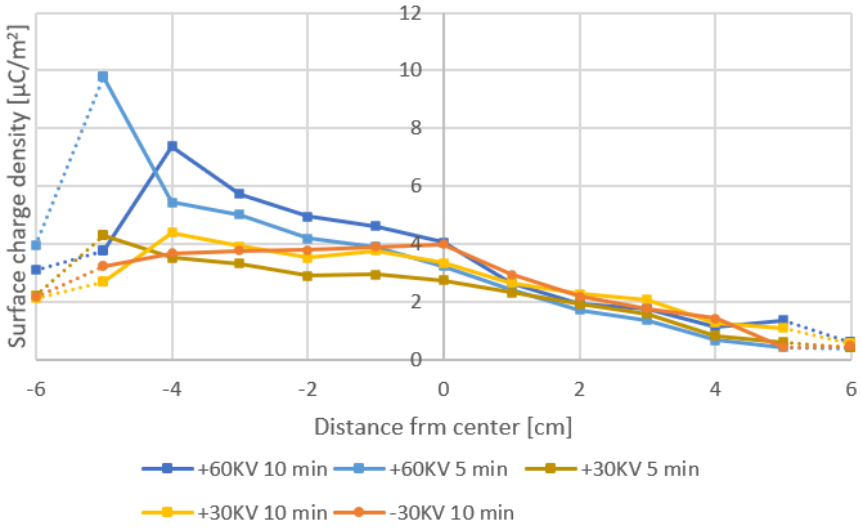

Figure 4.22: Surface charge density distribution comparison for different voltage levels

Based on previous plots, the magnitude was brought into comparison as seen in Figure 4.23. Based on the two blue bars for 60 kV, the magnitude measured to almost be the same even with double amount of charging time. However the peak did appear in different location of the test cell as one can see in Figure 4.21. For the data of 30 kV in Figure 4.23, one can notice a larger peak voltage for the negative polarity. This showed a concise indication on the effect of voltage polarity for this

particular test setup. However these magnitude difference was minor and certainly would not affect the performance of the test cell.

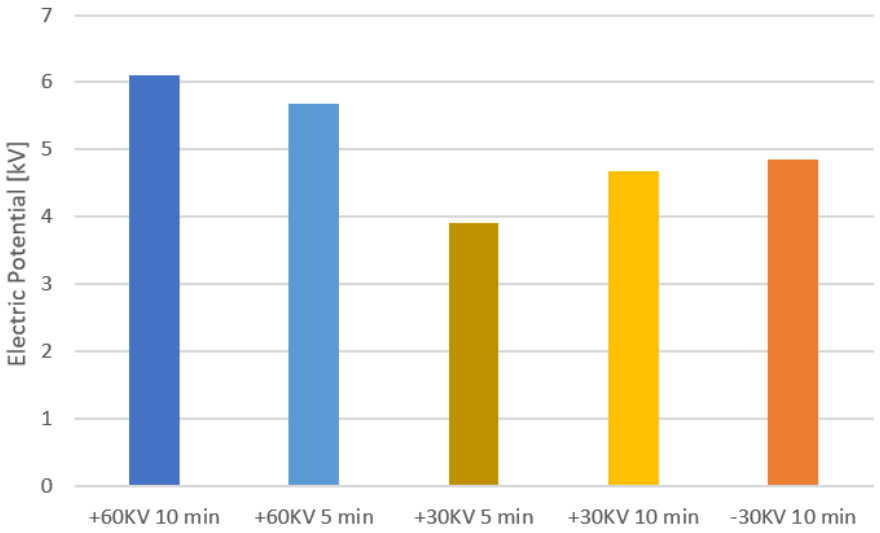

Figure 4.23: Amplitudes of each curve from Figure 4.21 into comparison

The information in Figure 4.24 support the statement above that even with the double amount of charging time, it would not be possible to measure double amount of surface potential therefore also double amount of surface charge density. The most consistent result of the 30 kV bars are the +30 kV for 10 min where the peaks were in reasonably fair range. However the highest peak of them are recorded from the negative polarity but with a less consistency. Since there were only three trials of each experiment one can not be certain that the negative polarity would give a higher voltage magnitude in the test cell. It is also shown in the Figure 4.24 that the double amount of charging time is not the double amount of surface potential, nor is it shown when looking the double amount of voltage charging level. Therefore it could be seen as a saturating charging behaviour of the experiment, the cause of this phenomena could be due to different factors such as the ambient condition. Since it was not measured before each experiment, different condition could affect the amount of surface charge inside the test cell.

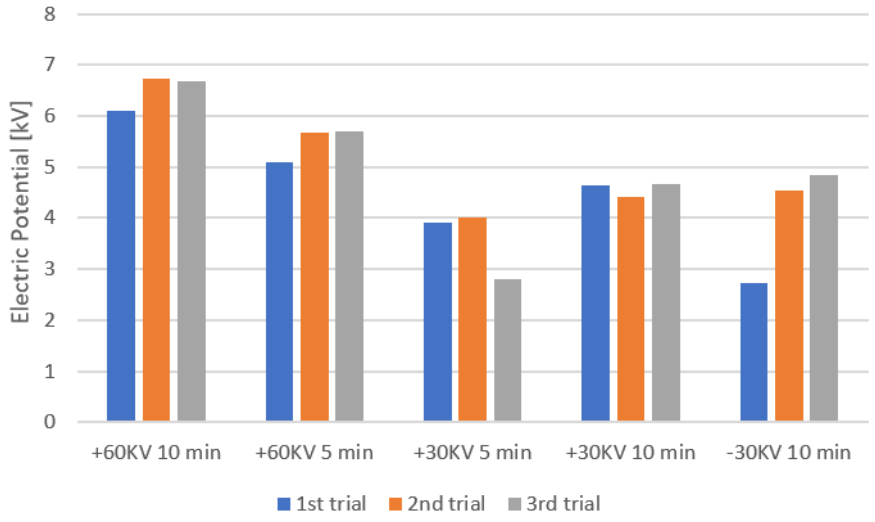

Figure 4.24: Amplitude comparison for all data from tangential field energizing behind silicone rubber plate

A rounded surface geometry was implemented into the test cell by physically applying force on the pressure plate. According to the simulation counter-part of this project, for negative voltage polarity, a tendency of charge accumulation at the gel surface near cavity formed by the rounded surface geometry has been recorded [13]. However the study could only present how the charges were accumulating for a few milliseconds after charging due to convergence limits. The data shown in Figure 4.25 illustrates a consistent measurements of higher voltages recorded from test of negative polarity. The difference in magnitude was calculated to be a difference of 16%, even though there was a time delay of about 10 to 15 seconds between energizing to grounding and measurement, one can still record a higher amplitude. However in the simulation counter-part studies the difference in magnitude between polarities is much larger due to corona discharges. In contrary to this study where the magnitude difference is slightly difference, since there was no corona discharges in the test cell when energizing through electrode. With a voltage of 60 kV and a distance between the polymer plates of 130 mm, the average field inside the test cell was 0.46 kV/mm which was far below the criterion of corona discharges of 3 kV/mm. Since there was no corona discharges inside the test cell but the negative voltage is still higher might be due to the free electrons in air. In general background radiation creates positive ions and electrons, the electrons will bind immediately to a neutral molecule creating negative ions. However for the produced electrons near the gel surface might travel towards the surface before it get to bind with a neutral molecule, creating negative surface charges.

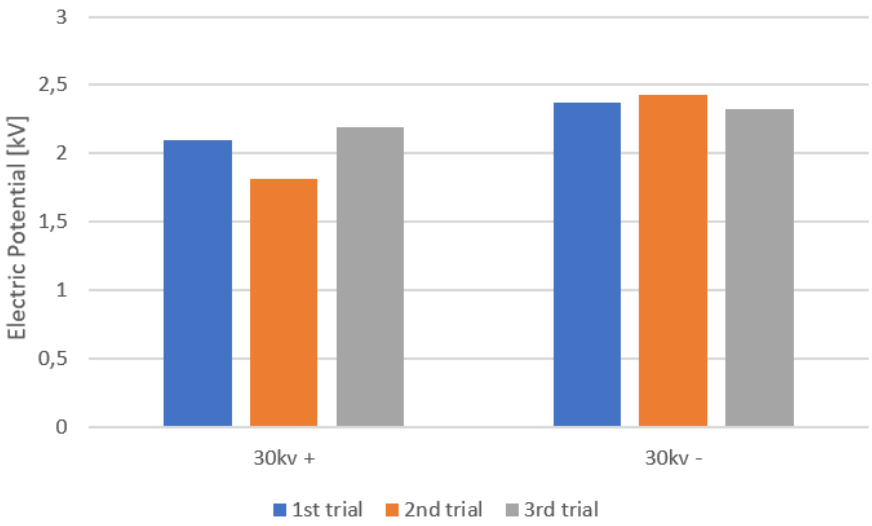

Figure 4.25: Polarity comparison at -5th element in rounded surface geometry composition

When the -5th element data from flat surface geometry was taken into comparison, one can generate a decay curve as seen in Figure 4.26.

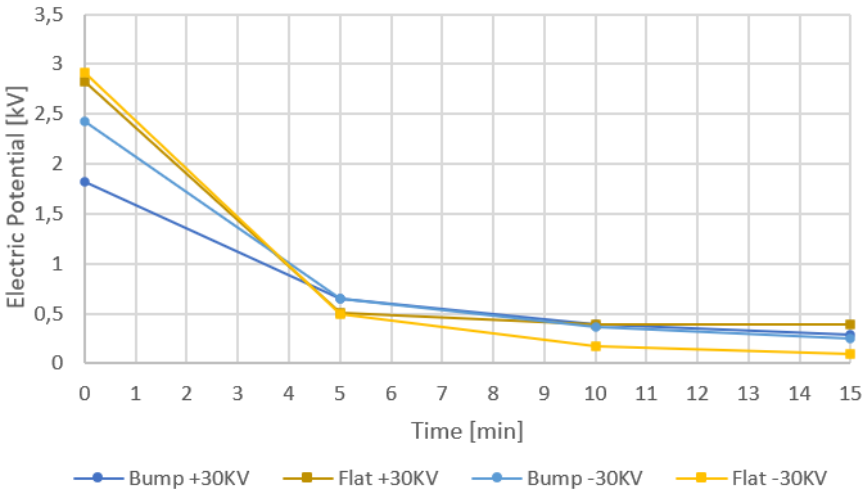

Figure 4.26: Decay curve at -5th element in the test cell for different charging settings and surface geometry.

There were some hypotheses that the angle in the triple point for rounded surface geometry, would create an internal electrical field between the gel surface and grounded electrode. this could explain the reason behind the lower recorded voltage at minute 0 for the rounded surface geometry. Nonetheless as stated in subsection 4.1.2, the potential decay rate is field depended, it did not show any larger difference in decay rate in Figure 4.27.

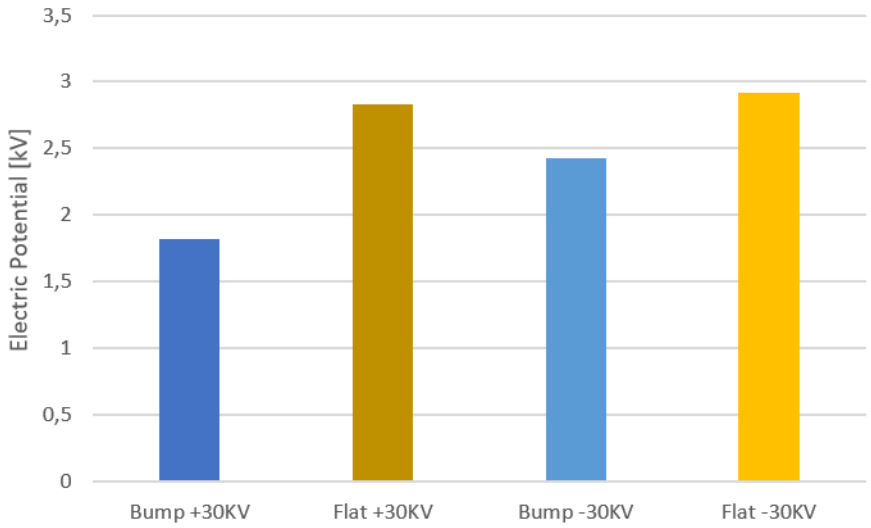

Figure 4.27: Comparison between different polarity and surface geometry of gel

For all the electric potential distribution that was presented so far seemed to be more or less consistent for all three trials. However there are few trials that did not reach up to the average voltage level, the most noticeable was the first trial for -30 kV 10 min as seen in Figure 4.24. There are many possible factors that could play its role, i.e. the amount of produced ions and electrons in air from radiation. It is also worth mentioning that in the test cell both SiR and GFR plate were grounded during measurements, and with the electric field zeroing technique in the probe, an extra charge decay mechanism may play in role. Since the probe will have the same potential as the gel surface, may result in an electric field between the probe and the plates when being near enough.

5

Conclusion

This project have conducted several experiment to understand charging and charge decay on the insulation gel, both for a grounded flat sample and a test cell which were supposed to resemble a section of a cable termination. The flat gel sample with corona charging from above gave an indication of charge decay characteristic whereas the test cell experiments showed the overall effects of the set up, i.e. how the surface geometry of the gel affects the charge location. But also how the surrounding materials had its impact of charge development.

The first experiments using corona charging on a flat uniform gel sample with its surface open to ambient air, where surface potential distribution and decay measurements were collected. The surface potential distribution were symmetrical with a few deviation with time which was influenced by the creases of aluminium foil beneath. Total time of potential decay (up to 10 kV charging) was about 8 to 10 hours and based on the decay measurement, some material characterisation of the gel could be found. The conductivity had a exponential field dependency around its data sheet value of $10^{-14} S/m$ as provided from the manufacturer. The gel also showed existence of energy traps around energy gap of 0.8 to 0.9 eV. The charge decay measurements on gel sample showed no significance dependency on polarity. The main decay mechanism of the gel sample were conduction through the bulk which was expected due to the different conductivity between the gel and air.

As for the corona charging inside the test cell through a needle above the gel surface, the distribution of charges were more or less uniform immediately after charging. However already after 5 min there were a difference in charge decay at each side of the test cell due to different conductivity of the SiR and GFR plate. At the SiR side the charges were more or less fully discharged after 15 minutes in contrary to the GFR side where the charges only had a 20% loss in magnitude.

When the energized electrode behind SiR plate was used, the charges near the SiR were decreasing with time. Instead, for the GFR region the amount of charges were slightly increasing. Based on the different voltage levels that were implemented into the experiment a non linear charging characteristic of the gel was identified. There were no significant influence from voltage polarity based on the observation that were made other than for the rounded surface geometry, where one recognized a slightly higher voltage of around 16% for the negative polarity than positive polarity. The surface charge density distribution was more center focused with time, where it was more pronounced after 10 to 15 minutes. Based on field calculations

in the test cell, there were a field enhancement at the triple junction of SiR, insulation gel and air. This field enhancement could possibly initiate local breakdown near the triple junction if the voltage is high enough. Although this experimental project only included energizing by pre-stressing which uses voltage levels far below flashover voltage level, a field enhancement is an indication of possible breakdown.

The presented results shows the material characteristic and charge dynamics of the gel inside the test cell, but also an indication of possible breakdown in which will contribute in the process of further development of the dry cable termination. The charging behaviour experiment of this type of test cell setup is of novelty and will contribute to the understanding of charge physics inside the cable termination for voltages under critical voltage level. In terms of development of the product, one may consider different optimization in order to diminish the unwanted surface charges inside the cable termination. One possible solution of improvement could be a larger cable termination, however with a larger products results in increased of direct and indirect cost which is not economical sustainable. Beyond increasing the overall size, one may consider changing the thickness of the polymers. Even then one has to take other factors into consideration such as mechanical strength.

6
Future works

Since there was only three trials for every experiment, one might need to extend it to 6 or more trials to ensure a statistical significance of results. A more in depth investigation might also be needed where the surrounding are more controlled such as ambient temperature or humidity, in such way the amount of ions in the air can be estimated.

To be able to localize the charge with precision, a scaled up version of the model may be suggested for future experiments. This allows the probe to reach in to the triple junction so that voltage estimation did not have to been made, which was needed to be done in this project. The area of interest has shown to be the triple junction due to local field enhancement in that area. There were also some discussion at the beginning of the project to use the ink from a printer to localize the charges, however due to the gelatinous character of the silicone gel, a different method of charge localizing might be needed. The field enhancement does not only indicated the possibility for breakdown inside the cable termination but also backs up parallel studies where it also have shown local field enhancement. However a further investigation is needed to confirm recent hypothesis, such as for positive polarity the voltage development was inside the silicone rubber [13]. Implementation of higher voltages including discharge physics is also of interest, where the amount of ions are generated locally.

Bibliography

[1] T.Sörqvist, A.Lundblad, and J.Svahn, "A unique dry 145 kv prefabricated one-piece self-supporting outdoor cable-termination," *International Conference on Insulated Power Cables*, vol. 10, pp. 1–6, 6 2019.

[2] Wacker, "Powersil® gel a/b," 2019.

[3] J. A. Giacometti and O. N. O. Jr., "Corona charging of polymers," *IEEE Transactions on Electrical Insulation*, no. 5, pp. 924–944, 1992.

[4] S. Kumara, "Electrical charges on polymeric insulator surfaces and their impact on flashover performances," Ph.D. dissertation, Chalmers University of Technology, Gothenburg, Sweden, 2012.

[5] N. Jonassen, *Electrostatic*. Kluwer Academic Publishers, 2002.

[6] S. Alam, "Surface charge dynamics on polymeric insulating materials for high voltage applications," 2014.

[7] D. C. Faircloth and N. L. Allen, "High resolution measurements of surface charge densities on insulator surfaces," *IEEE*, vol. 10, no. 2, pp. 285–290, 04 2003.

[8] S.Kumara, Y. V. Serdyuk, and S. M. Gubanski, "Surface charge decay on polymeric materials under different neutralization modes in air," *IEEE*, vol. 18, no. 5, pp. 1779–1788, 10 2011.

[9] G. M. Ieda and U.Shinohara, "A decay process of surface electric charges across polyethylene film," *Japan. J. Appl. Phy*, no. 6, pp. 739–734, 1967.

[10] E. Seran, M. Godefroy, E. Pili, N. Michielsen, and S. Bondiguel., "What we can learn from measurements of air electric conductivity in 222rn-rich atmosphere," *Earth and Space Science*, 2 2017.

[11] S. D. Pawar and P. Murugavel, "Effect of relative humidity and sea level pressure on electrical conductivity of air over indian ocean," *JOURNAL OF GEOPHYSICAL RESEARCH*, no. 114, pp. 1–8, 1 2009.

[12] S. Kumara, Y. V. Serdyuk, S. M. Gubanski, S. Alam, and I. R. Hoque, "Dc flashover characteristics of a polymeric insulator in presence of surface charges," *IEEE Transactions on Dielectrics and Electrical Insulation*, no. 3, pp. 1084–1090, 1 2012.

[13] S. Chenxuan, "Simulation of charging behavior on surfaces of polymeric insulation inside hvac cable termination," 2020.